sor protein is associated with increased levels of transthyretin and the activation of cell survival pathways. *J. Neurosci.* **22,** 7380–7388
30. Taguchi, A., Wartschow, L. M., and White, M. F. (2007) Brain IRS2 signaling coordinates life span and nutrient homeostasis. *Science* **317,** 369–372
31. Selman, C., Lingard, S., Choudhury, A. I., Batterham, R. L., Claret, M., Clements, M., Ramadani, F., Okkenhaug, K., Schuster, E., Blanc, E., Piper, M. D., Al Qassab, H., Speakman, J. R., Carmignac, D., Robinson, I. C., Thornton, J. M., Gems, D., Partridge, L., and Withers, D. J. (2008) Evidence for lifespan extension and delayed age-related biomarkers in insulin receptor substrate 1 null mice. *FASEB J.* **22,** 807–818
32. Leissring, M. A., Farris, W., Chang, A. Y., Walsh, D. M., Wu, X., Sun, X., Frosch, M. P., and Selkoe, D. J. (2003) Enhanced proteolysis of beta-amyloid in APP transgenic mice prevents plaque formation, secondary pathology, and premature death. *Neuron* **40,** 1087–1093
33. Burks, D. J., de Mora, J. F., Schubert, M., Withers, D. J., Myers, M. G., Towery, H. H., Altamuro, S. L., Flint, C. L., and White, M. F. (2000) IRS-2 pathways integrate female reproduction and energy homeostasis. *Nature* **407,** 377–382
34. Adlerz, L., Holback, S., Multhaup, G., and Iverfeldt, K. (2007) IGF-1-induced processing of the amyloid precursor protein family is mediated by different signaling pathways. *J. Biol. Chem.* **282,** 10203–10209
35. Costantini, C., Scrable, H., and Puglielli, L. (2006) An aging pathway controls the TrkA to p75NTR receptor switch and amyloid beta-peptide generation. *EMBO J.* **25,** 1997–2006
36. McConlogue, L., Buttini, M., Anderson, J. P., Brigham, E. F., Chen, K. S., Freedman, S. B., Games, D., Johnson-Wood, K., Lee, M., Zeller, M., Liu, W., Motter, R., and Sinha, S. (2007) Partial reduction of BACE1 has dramatic effects on Alzheimer plaque and synaptic pathology in APP transgenic mice. *J. Biol. Chem.* **282,** 26326–26334
37. Ronnemaa, E., Zethelius, B., Sundelof, J., Sundstrom, J., Degerman-Gunnarsson, M., Berne, C., Lannfelt, L., and Kilander, L. (2008) Impaired insulin secretion increases the risk of Alzheimer disease. *Neurology* **71,** 1065–1071
38. Whitmer, R. A., Selby, J. V., Van Den Eeden, S. K., Haan, M. N., Quesenberry, Jr., C. P., Minkoff, J., and Yaffe, K. (2006) Glycemic control and risk of dementia in a cohort of patients with type 2 diabetes. *Alzheimers Dement.* **2,** S149
39. Cukierman-Yaffe, T., Gerstein, H. C., Williamson, J. D., Lazar, R. M., Lovato, L., Miller, M. E., Coker, L. H., Murray, A., Sullivan, M. D., Marcovina, S. M., and Launer, L. J. (2009) Relationship between baseline glycemic control and cognitive function in individuals with type 2 diabetes and other cardiovascular risk factors: the action to control cardiovascular risk in diabetes-memory in diabetes (ACCORD-MIND) trial. *Diabetes Care* **32,** 221–226
40. Doria, A., Patti, M. E., and Kahn, C. R. (2008) The emerging genetic architecture of type 2 diabetes. *Cell. Metab.* **8,** 186–200
41. Vardy, E. R., Rice, P. J., Bowie, P. C., Holmes, J. D., Grant, P. J., and Hooper, N. M. (2007) Increased circulating insulin-like growth factor-1 in late-onset Alzheimer's disease. *J. Alzheimers Dis.* **12,** 285–290
42. Wolkow, C. A., Kimura, K. D., Lee, M. S., and Ruvkun, G. (2000) Regulation of C. elegans life-span by insulin-like signaling in the nervous system. *Science* **290,** 147–150
43. Holzenberger, M., Dupont, J., Ducos, B., Leneuve, P., Geloen, A., Even, P. C., Cervera, P., and Le Bouc, Y. (2003) IGF-1 receptor regulates lifespan and resistance to oxidative stress in mice. *Nature* **421,** 182–187
44. Kappeler, L., Filho, C. M., Dupont, J., Leneuve, P., Cervera, P., Perin, L., Loudes, C., Blaise, A., Klein, R., Epelbaum, J., Le Bouc, Y., and Holzenberger, M. (2008) Brain IGF-1 receptors control mammalian growth and lifespan through a neuroendocrine mechanism. *PLoS Biol.* **6,** e254
45. Kang, J., Lemaire, H. G., Unterbeck, A., Salbaum, J. M., Masters, C. L., Grzeschik, K. H., Multhaup, G., Beyreuther, K., and Muller-Hill, B. (1987) The precursor of Alzheimer's disease amyloid A4 protein resembles a cell-surface receptor. *Nature* **325,** 733–736
46. Vassar, R., Bennett, B. D., Babu-Khan, S., Kahn, S., Mendiaz, E. A., Denis, P., Teplow, D. B., Ross, S., Amarante, P., Loeloff, R., Luo, Y., Fisher, S., Fuller, J., Edenson, S., Lile, J., Jarosinski, M. A., Biere, A. L., Curran, E., Burgess, T., Louis, J. C., Collins, F., Treanor, J., Rogers, G., and Citron, M. (1999) Beta-secretase cleavage of Alzheimer's amyloid precursor protein by the transmembrane aspartic protease BACE. *Science* **286,** 735–741
47. Lorenzo, A., and Yankner, B. A. (1994) Beta-amyloid neurotoxicity requires fibril formation and is inhibited by Congo red. *Proc. Natl. Acad. Sci. U. S. A.* **91,** 12243–12247
48. Lammich, S., Kojro, E., Postina, R., Gilbert, S., Pfeiffer, R., Jasionowski, M., Haass, C., and Fahrenholz, F. (1999) Constitutive and regulated alpha-secretase cleavage of Alzheimer's amyloid precursor protein by a disintegrin metalloprotease. *Proc. Natl. Acad. Sci. U. S. A.* **96,** 3922–3927
49. Puglielli, L. (2008) Aging of the brain, neurotrophin signaling, and Alzheimer's disease: is IGF1-R the common culprit? *Neurobiol. Aging* **29,** 795–811
50. Puglielli, L., Ellis, B. C., Saunders, A. J., and Kovacs, D. M. (2003) Ceramide stabilizes beta-site amyloid precursor protein-cleaving enzyme 1 and promotes amyloid beta-peptide biogenesis. *J. Biol. Chem.* **278,** 19777–19783
51. Meilandt, W. J., Cisse, M., Ho, K., Wu, T., Esposito, L. A., Scearce-Levie, K., Cheng, I. H., Yu, G. Q., and Mucke, L. (2009) Neprilysin overexpression inhibits plaque formation but fails to reduce pathogenic Aβ oligomers and associated cognitive deficits in human amyloid precursor protein transgenic mice. *J. Neurosci.* **29,** 1977–1986
52. Zhao, L., Teter, B., Morihara, T., Lim, G. P., Ambegaokar, S. S., Ubeda, O. J., Frautschy, S. A., and Cole, G. M. (2004) Insulin-degrading enzyme as a downstream target of insulin receptor signaling cascade: implications for Alzheimer's disease intervention. *J. Neurosci.* **24,** 11120–11126
53. Hill, J. M., Lesniak, M. A., Pert, C. B., and Roth, J. (1986) Autoradiographic localization of insulin receptors in rat brain: prominence in olfactory and limbic areas. *Neuroscience* **17,** 1127–1138
54. Van Houten, M., and Posner, B. I. (1979) Insulin binds to brain blood vessels in vivo. *Nature* **282,** 623–625
55. Van Houten, M., and Posner, B. I. (1983) Circumventricular organs: receptors and mediators of direct peptide hormone action on brain. *Adv. Metab. Disord.* **10,** 269–289
56. Baskin, D. G., Davidson, D., Corp, E. S., Lewellen, T., and Graham, M. (1986) An inexpensive microcomputer digital imaging system for densitometry: quantitative autoradiography of insulin receptors with 125I and LKB ultrofilm. *J. Neurosci. Methods* **16,** 119–129
57. Unger, J., McNeill, T. H., Moxley, R. T., III, White, M., Moss, A., and Livingston, J. N. (1989) Distribution of insulin receptor-like immunoreactivity in the rat forebrain. *Neuroscience* **31,** 143–157
58. Werther, G. A., Hogg, A., Oldfield, B. J., McKinley, M. J., Figdor, R., Allen, A. M., and Mendelsohn, F. A. (1987) Localization and characterization of insulin receptors in rat brain and pituitary gland using in vitro autoradiography and computerized densitometry. *Endocrinology* **121,** 1562–1570
59. Schulingkamp, R. J., Pagano, T. C., Hung, D., and Raffa, R. B. (2000) Insulin receptors and insulin action in the brain: review and clinical implications. *Neurosci. Biobehav. Rev.* **24,** 855–872
60. Reger, M. A., Watson, G. S., Green, P. S., Wilkinson, C. W., Baker, L. D., Cholerton, B., Fishel, M. A., Plymate, S. R., Breitner, J. C., DeGroodt, W., Mehta, P., and Craft, S. (2008) Intranasal insulin improves cognition and modulates beta-amyloid in early AD. *Neurology* **70,** 440–448
61. Niedernhofer, L. J., Garinis, G. A., Raams, A., Lalai, A. S., Robinson, A. R., Appeldoorn, E., Odijk, H., Oostendorp, R., Ahmad, A., van Leeuwen, W., Theil, A. F., Vermeulen, W., van der Horst, G. T., Meinecke, P., Kleijer, W. J., Vijg, J., Jaspers, N. G., and Hoeijmakers, J. H. (2006) A new progeroid syndrome reveals that genotoxic stress suppresses the somatotroph axis. *Nature* **444,** 1038–1043

Received for publication March 16, 2009.
Accepted for publication May 7, 2009.

Research Article

Journal of Applied Toxicology

Received: 6 April 2009, Revised: 7 May 2009, Accepted 2 June 2009, Published online in Wiley InterScience: 21 July 2009

(www.interscience.wiley.com) DOI 10.1002/jat.1459

Aryl hydrocarbon receptor-mediated effects of 2,3,7,8-tetrachlorodibenzo-*p*-dioxin on glucose-stimulated insulin secretion in mice

Hisaka Kurita,[a] Wataru Yoshioka,[a] Noriko Nishimura,[b] Naoto Kubota,[c,d] Takashi Kadowaki[c] and Chiharu Tohyama[a,b]*

ABSTRACT: Epidemiological and laboratory studies suggested that exposure to 2,3,7,8-tetrachlorodibenzo-*p*-dioxin (TCDD) affects glucose homeostasis and increases the incidence of type 2 diabetes mellitus. To evaluate the effects of TCDD on insulin secretion from islets of Langerhans (islets), we designed *in vivo*, *ex vivo* and *in vitro* experiments. For the *in vivo* experiment, male C57BL/6J and aryl hydrocarbon receptor (AhR)-null mice were injected intraperitoneally with TCDD (10 μg kg^{-1} b.w.), fasted for 12 h and administered glucose 24 h post-administration. TCDD exposure significantly decreased the plasma insulin concentration at 60 and 120 min after a glucose challenge in C57BL/6J mice but not in AhR-null mice. In contrast, the plasma glucose concentration was not changed by TCDD exposure in both C57BL/6J and AhR-null mice. For the *ex vivo* experiment, we isolated islets 24 h after TCDD administration and determined the glucose-stimulated insulin secretion from the islets. The insulin secretion level was found to be significantly decreased by TCDD exposure at 60 min after glucose treatment. For the *in vitro* experiment, islets harvested from untreated C57BL/6J mice were exposed to 0.1, 1, 10 or 100 nM TCDD for 24 h and analyzed for glucose-stimulated insulin secretion. Insulin secretion from the islets remained unchanged regardless of TCDD dose. In conclusion, TCDD exposure impaired the second phase of glucose-stimulated secretion of insulin from the islets via the AhR signaling pathway. Copyright © 2009 John Wiley & Sons, Ltd.

Keywords: aryl hydrocarbon receptor; dioxin; glucose; insulin; islets of Langerhans

INTRODUCTION

The incidence of obesity and its related disease state, such as type 2 diabetes, has considerably increased in industrialized societies owing to lifestyle changes, such as high calorie intake and lack of physical exercise. It has been estimated that the number of type 2 diabetic patients will increase to 366 million worldwide by 2030 (Wild *et al.*, 2004), and that the high incidence of type 2 diabetes is becoming a serious medical and social problem that needs to be addressed to ensure a better quality of life for the overwhelmingly increasing aged population. Type 2 diabetes is characterized by impaired insulin secretion from the islets of Langerhans and insulin resistance in the target organs such as liver, adipose tissue and muscle (Porte, 2001). It is established that the dysfunction of pancreatic β cells is accompanied by impaired insulin secretion, and intricately associated with chronic hyperglycemia and insulin resistance (Kahn *et al.*, 2006).

Epidemiological studies suggest that, besides hereditary factors, the impairment of insulin secretion could be induced by exposure to environmental pollutants. For example, American war veterans who were engaged in the operation to spray defoliant containing 2,3,7,8-tetrachlorodibenzo-*p*-dioxin (TCDD) during the Vietnam War showed that the levels of TCDD exposure correlate significantly with the incidence of type 2 diabetes (Michalek *et al.*, 1999). The results of the third National Health and Nutrition Examination Survey (NHANES III) in the USA suggested that the urinary cadmium level is significantly associated with the fasting glucose level and type 2 diabetes in adults older than 40 years in age (Schwartz *et al.*, 2003). On the other hand, experiments using rodents showed that exposure to cadmium (Ithakissios *et al.*, 1975), methylmercury (Chen *et al.*, 2006) and TCDD (Novelli *et al.*, 2005) decreases plasma insulin concentrations or the level of insulin secretion from the islets, suggesting that exposure to environmental pollutants may increase the incidence of type 2 diabetes.

Among these chemicals, TCDD has been known to bind to a receptor, named aryl hydrocarbon receptor (AhR) that is known to be present in many types of cells from nematodes to mammals (Butler *et al.*, 2001; Hahn *et al.*, 1997). This receptor has an

*Correspondence to: C. Tohyama, Laboratory of Environmental Health Sciences, Center for disease Biology and Integrative Medicine, Graduate School of Medicine, The University of Tokyo, 7-3-1 Hongo, Bunkyo-ku, Tokyo 113-0033, Japan.
Email: mtohyama@mail.ecc.u-tokyo.ac.jp

[a]Laboratory of Environmental Health Sciences, Center for Disease Biology and Integrative Medicine, Graduate School of Medicine, The University of Tokyo, Tokyo, Japan

[b]Research Center for Environmental Risk, National Institute for Environmental Studies, Tokyo, Japan

[c]Department of Metabolic Diseases, Graduate School of Medicine, The University of Tokyo, Tokyo, Japan

[d]Translational Systems Biology and Medicine Initiative, Graduate School of Medicine, The University of Tokyo, Tokyo, Japan

extremely high affinity for TCDD. Thus, we selected TCDD as a model compound to study the toxicity mechanism associated with glucose tolerance and insulin secretion from the islets. Once TCDD binds to AhR in the cytoplasm, the TCDD-AhR complex can be translocated into the nucleus, and forms a heterodimer with AhR nuclear translocator (Arnt). This liganded transcription factor complex binds to the xenobiotic-responsive element in the promoter region of target genes, which will accelerate transcriptional activity and induce biological responses or toxicities (Gonzalez and Fernandez-Salguero, 1998). Although AhR-null mice did not develop TCDD-induced toxicities and disease states, such as hydronephrosis, cleft palate and thymic atrophy (Fernandez-Salguero *et al.*, 1996; Mimura *et al.*, 1997), it has not been determined whether the TCDD-induced effects on glucose homeostasis are mediated by AhR. Insulin secretion was found to be decreased by TCDD exposure in the rat (Novelli *et al.*, 2005; Piaggi *et al.*, 2007), but whether TCDD-induced suppression of insulin secretion is mediated by AhR is not known. In the present study, we examined the effects of TCDD on glucose-stimulated insulin release by *in vivo*, *ex vivo* and *in vitro* experiments, and investigated the importance of AhR in TCDD-dependent disruption of glucose homeostasis, such as insulin secretion from the islets by using AhR-null mice.

MATERIALS AND METHODS

Animals

Male C57BL/6J strain mice were purchased from CLEA Japan, Inc. (Tokyo, Japan). AhR(−/−) mice (Mimura *et al.*, 1997) were a kind gift from Dr Y. Fujii-Kuriyama. The male AhR(+/−) were backcrossed 13 times to female C57BL/6J mice, and AhR(−/−) mice were produced by mating heterozygous AhR transgenic mice at the National Institute for Environmental Studies. The genotype of each pup was determined by analyzing the presence of the mutant AhR allele by PCR with genomic DNA in a tissue taken from the tail. The mice were housed in a room with temperature at 23 ± 1°C and humidity at 50 ± 10%, on a 12/12 h light–dark cycle. Laboratory rodent chow (Labo MR Stock, Nosan, Yokohama, Japan) and distilled water were provided *ad libitum*. The experimental protocols using the mice were approved by the Animal Care Committee of the Graduate School of Medicine, the University of Tokyo.

In Vivo Experiment: Oral Glucose Tolerance Test

TCDD (purity >99.5%; Cambridge Isotope Laboratory, Andover, MA, USA) was dissolved in corn oil (Wako Pure Chemicals, Osaka, Japan). The corn oil containing 2% *n*-nonane (Nacalai Tesque, Kyoto, Japan) was used for vehicle (control) treatment. Male C57BL/6J and AhR-null 8-week-old mice were injected intraperitoneally with a single dose of vehicle (control) or TCDD (10 μg kg^{-1} b.w.). Twelve hours after TCDD treatment, the mice were fasted for a further 12 h and administered glucose solution at a single oral dose of 2.0 g kg^{-1} b.w. Blood was collected from the tail vein at 0, 15, 30, 60 and 120 min after glucose administration, followed by separation of plasma. Insulin in the plasma was determined using mouse insulin enzyme-linked immunosorbent assay (ELISA) (AKRIN-011, Shibayagi, Shibukawa, Japan). Plasma glucose was determined using a GLU-PIII test slide (Fujifilm, Asaka, Japan).

Ex Vivo Experiment: Insulin Release from the Isolated Islets

Twenty-four hours after the intraperitoneal injection of TCDD, C57BL/6J mice were lightly anesthetized with diethyl ether. Islets were isolated by collagenase digestion. In brief, after clamping the common bile duct at a point close to the duodenal outlet, collagenase (Liberase RI, Roche Applied Science, Indianapolis, IN, USA) was injected into the duct. The swollen pancreas was removed and incubated at 37 °C for 24 min. The pancreas was dispersed by pipetting and washed three times with buffer [Hank's balanced salt solution with 25 mM HEPES (pH 7.4) and 10% newborn calf serum]. Islets were manually collected under a microscope. The isolated islets were incubated in DMEM supplemented with 10% newborn calf serum for 12 h under 5% CO_2 at 37 °C. Groups of islets (seven islets per sample) were incubated for 0, 10 or 60 min at 37 °C in 0.5 ml of Krebs–Ringer bicarbonate buffer (KRB) supplemented with 22.4 mM glucose and 0.2% bovine serum albumin (BSA). Supernatants were collected for insulin determination. To determine insulin inside the islets, the islets were treated with 0.5 ml of acidified ethanol (29:7:3, v/v, 99.5% ethanol:H_2O:5.0 M HCl) kept frozen at -20 °C until ELISA for insulin.

In Vitro Experiment: Insulin Release from Isolated Islets

Islets were isolated from untreated C57BL/6J mice by collagenase digestion as described in '*Ex vivo* experiment' and incubated in DMEM under 5% CO_2 at 37 °C for 12 h. Groups of islets (seven islets per sample) were incubated in 0.5 ml of DMEM containing 0, 0.1, 1, 10 or 100 nM TCDD under 5% CO_2 at 37 °C for 24 h. After TCDD exposure, the islets were washed with KRB and incubated in KRB containing 22.4 mM glucose and 0.2% BSA at 37 °C for 60 min. The medium containing the islets was centrifuged to separate the supernatant and islets for insulin determination by ELISA.

Statistical Analysis

All the results are expressed as mean ± SEM. Data between groups were compared using Student's *t*-test or one-way ANOVA with *post hoc* analysis by Bonferroni's test. A *P*-value of less than 0.05 was considered statistically significant.

RESULTS

In Vivo Experiment

To examine the effects of TCDD on glucose metabolism, we performed *in vivo* oral glucose tolerance test (OGTT). In this experiment, C57BL/6J and AhR-null mice were used to evaluate the possible involvement of AhR in the TCDD-induced effects. Plasma insulin concentrations at 60 and 120 min after glucose challenge were significantly decreased by TCDD exposure in C57BL/6J mice [Fig. 1(A)], whereas in AhR-null mice, no difference in plasma insulin concentrations was observed until 120 min after glucose administration [Fig. 1(B)]. In contrast, TCDD exposure did not alter the plasma glucose concentrations in both C57BL/6J and AhR-null mice (Fig. 2). These results indicate that the impaired insulin secretion following TCDD administration was mediated in an AhR-dependent manner.

Journal of AppliedToxicology

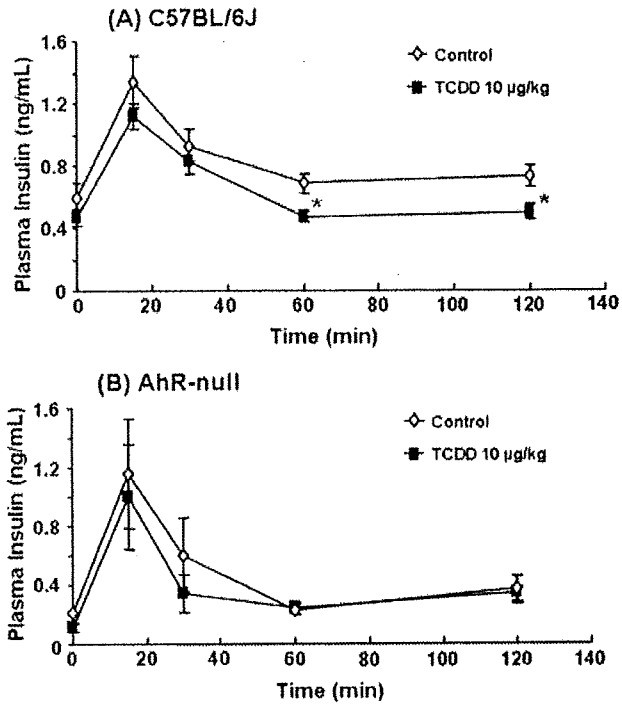

Figure 1. Plasma insulin level after a glucose challenge in C57BL/6J mice ($n = 10$ per group) (A) and AhR-null mice ($n = 4$ per group) (B) at 24 h after an intraperitoneal injection of TCDD at a dose of 10 μg kg^{-1} b.w. Data are expressed as mean ± SEM. *$P < 0.05$ as compared with control group at each time point (Student's t-test).

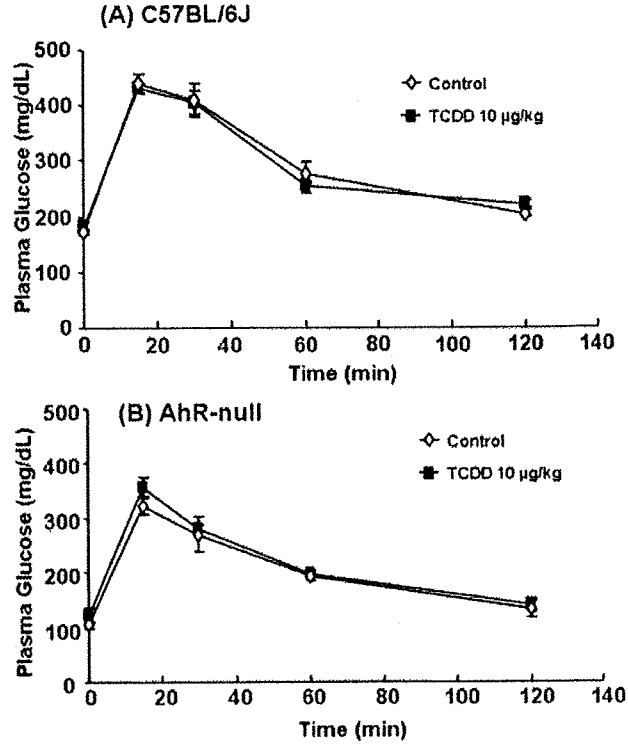

Figure 2. Plasma glucose level after a glucose challenge in C57BL/6J mice ($n = 10$ per group) (A) and AhR-null mice ($n = 4$ per group) (B) at 24 h after an intraperitoneal injection of TCDD at a dose of 10 μg kg^{-1} b.w. See also the legend to Fig. 1.

Ex Vivo Experiment

Because TCDD decreased the glucose-stimulated plasma insulin concentrations in C57BL/6J mice [Fig. 1(A)], we determined whether TCDD exposure affects glucose-stimulated insulin secretion using the isolated islets of C57BL/6J mice exposed to TCDD. The concentration of insulin released into the medium was not different between the control and TCDD-exposed islets at 10 min after glucose treatment, but was significantly decreased by TCDD exposure at 60 min after glucose treatment [Fig. 3(A)]. Under this experimental condition, the insulin contents of the islets were also significantly decreased by TCDD exposure at 60 min after glucose stimulation [Fig. 3(B)]. Although no statistically significant differences were found between the control and TCDD-exposed mice at 0 and 10 min after glucose stimulation, the insulin contents in control mice tended to be less than those in TCDD-exposed mice [Fig. 3(B)].

In Vitro Experiment

To evaluate the direct effects of TCDD on the glucose-stimulated insulin secretion, pancreatic islets were isolated first and then exposed to different concentrations of TCDD. Unlike in the *in vivo* TCDD exposure experiment, insulin secretion from the islets remained unchanged regardless of TCDD dose [Fig. 4(A)], although the insulin contents in the islets were significantly decreased at as low as 0.1 nM TCDD [Fig. 4(B)].

DISCUSSION

The impaired insulin secretion from the pancreatic islets following TCDD exposure shown in this study may support the previous epidemiological observations on the relationship between TCDD exposure and occurrence of diabetes mellitus. In a series of follow-up epidemiological studies on the health status of US Air Force veterans who were engaged in the spraying of defoliant containing TCDD during the Vietnam War, serum TCDD concentrations were suggested to be significantly associated with the prevalence of type 2 diabetes (Henriksen *et al.*, 1997) and insulin resistance (Kern *et al.*, 2004). Recently, such associations between TCDD and diabetes in Vietnam War veterans were strengthened after adjustments for calendar period, day of spraying defoliants, and time spent in Vietnam (Michalek and Pavuk, 2008). In other cohort studies on people exposed to excessively large amounts of TCDD in Seveso, Italy, mortality ascribed to diabetes was found to be significantly elevated (Bertazzi *et al.*, 1998; Pesatori *et al.*, 2003). The significant association of increased incidence of diabetes with exposure to TCDD was also reported in workers who were engaged in manufacturing phenoxyacid herbicide and chlorophenol (Vena *et al.*, 1998). These epidemiological observations are supported by several experimental studies. Exposure to TCDD was found to affect glucose metabolism such as a decrease in glucose uptake by the pancreas and adipose tissue in the guinea pig (Enan *et al.*, 1992) and an alteration of gluconeogenesis and PEPCK activity in the rat (Weber *et al.*, 1991). Other

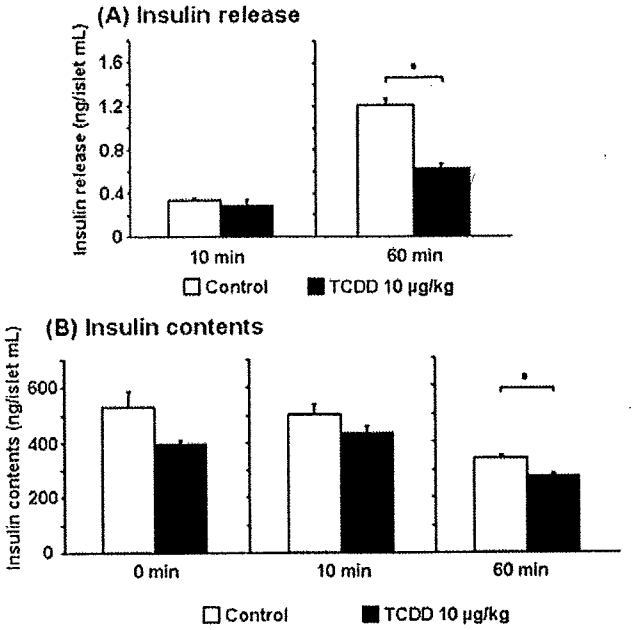

Figure 3. Insulin release (A) and contents (B) in islets stimulated with 22.4 mM glucose for 0, 10, 60 min, the islets were isolated from C57BL/6J mice at 24 h after an intraperitoneal injection of TCDD at a dose of 10 μg kg^{-1} b.w. Seven islets were grouped into one sample ($n = 5$–10 per group). See also the legend to Fig. 1.

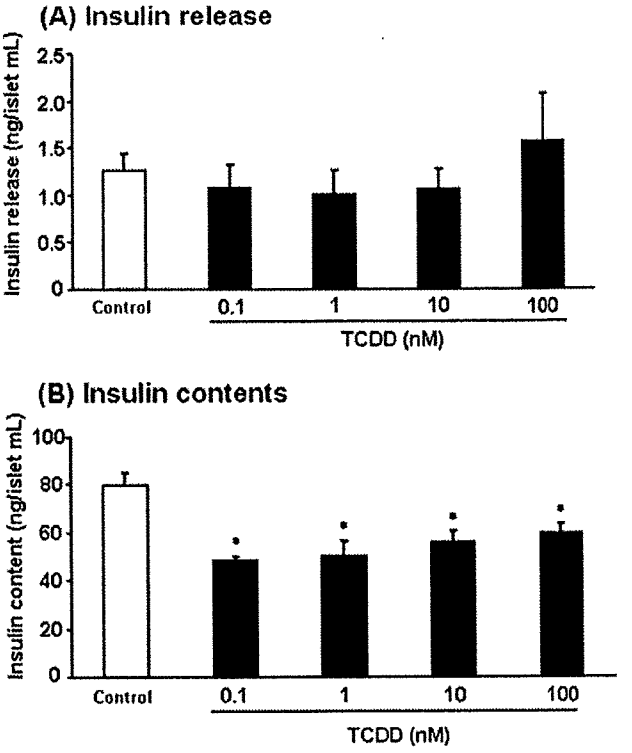

Figure 4. Insulin release (A) and contents (B) in islets stimulated with 22.4 mM glucose for 60 min after exposure to 0.1–100 nM TCDD for 24 h, the islets were isolated from intact C57BL/6J mice. Seven islets were grouped into one sample ($n = 5$ per group). Data are expressed as mean ± SEM. *$P < 0.05$ as compared with control group (one-way ANOVA, followed by *post hoc* Bonferroni's test).

studies also reported the effects of TCDD on glucose metabolism, including impairment of insulin secretion in rats (Novelli *et al.*, 2005) and glucose tolerance in mice (Ishida *et al.*, 2005).

In our present study, C57BL/6J mice exposed to TCDD at a dose of 10 μg kg^{-1} b.w. were found to have a decreased level of insulin secretion [Fig. 1(A)] but no impaired glucose tolerance [Fig. 2(A)]. The observation concerning insulin secretion supports the previous study using rats (Novelli *et al.*, 2005), but the observation concerning glucose tolerance is not consistent with the observation described in the above-mentioned study (Ishida *et al.*, 2005), in which the glucose tolerance was impaired on day 10 after an administration of a very high TCDD dose (100 μg kg^{-1} b.w.) that can induce wasting syndrome. It is considered that the difference between our study and the study by Ishida and coworkers ((Ishida *et al.*, 2005) could be due to a difference in the TCDD dosage or the selected time point. Thus, it is possible that glucose tolerance and insulin resistance could be developed if a slightly abnormal insulin secretion persists for a long period, and this hypothesis could be validated by chronic toxicity studies.

Previous studies have proposed some toxic mechanisms of insulin secretion induced by environmental pollutants. Cadmium, methylmercury and TCDD affect the calcium channels in the islets (Jijakli and Malaisse, 1998), PI3K/Akt signaling pathway (Chen *et al.*, 2006) and the production of ROS (Piaggi *et al.*, 2007), respectively. Nevertheless, how TCDD impairs insulin secretion at the molecular level is still unclear. There are several lines of experimental evidence that AhR and Arnt play physiological roles in glucose homeostasis. When female AhR-null mice were maintained for seven months, the mice were found to have a decreased plasma insulin level under fasting conditions and insulin resistance (Thackaberry *et al.*, 2003). In another study (Gunton *et al.*, 2005), type 2 diabetes patients were found to have a decreased level of Arnt expression in the pancreatic islets. In the Gunton and coworkers' study using Arnt-knocked-down MIN6 cells and β cell-specific Arnt-null mice, MODY gene (hepatocyte nuclear factor 4α), glucose-metabolism-related enzyme genes (glucose-6-phospho-isomerase, aldolase and phosphofructokinase) and insulin-signaling gene (Akt2) were down-regulated in accordance with impaired insulin secretion. Thus, it is considered that the AhR–Arnt signaling pathway may modulate insulin secretion through the regulation of the above-described genes that are associated with glucose homeostasis. On the other hand, we found that TCDD exposure impairs insulin secretion through an AhR signaling pathway [Fig. 1(B)]. How AhR or Arnt plays a regulatory role in insulin secretion remains to be studied.

Insulin is secreted from the islets in a biphasic fashion (Aizawa and Komatsu, 2005). In the first phase, insulin is rapidly secreted from the islets within 2 min upon glucose stimulation, followed by a gradual decrease within 10 min. This insulin secretion which is characterized by the fusion of insulin-containing granules, a readily releasable pool (RRP), with the cellular membrane, is caused by an increase in the intracellular Ca^{2+} concentration $[Ca^{2+}]_i$ triggered by the closure of ATP-sensitive K^+ (K_{ATP}) channel that is activated by glucose stimulation. In the second phase, the

insulin secretion level gradually increases after the first phase is nearly terminated. The second phase is characterized by the replenishment of RRP with insulin granules that are present in a reserve pool (RP). Although male Sprague–Dawley rats injected intraperitoneally with TCDD at a dose of 1 μg kg^{-1} b.w. showed decreased glucose uptake in the pancreas without alteration in the glucose transporter 2 protein level in the islets at 24 h post-administration (Novelli *et al.*, 2005), how insulin secretion was altered by TCDD is still unknown. In the present study, TCDD exposure *in vivo* and *ex vivo* decreased the level of insulin secretion from the islets [Figs 3(B) and 4(B)], but that *in vitro* did not [Figs 1(A), 3(A) and 4(A)]. These results suggest that the decrease of the insulin secretion level by TCDD is achieved in an indirect manner, presumably owing to its actions on other tissues. For instance, it has been reported that the removal of the ventromedial hypothalamus (VMH) elevates the insulin secretion (Berthoud and Jeanrenaud, 1979) and that exposure to TCDD of the rats whose VMH was surgically removed suppresses the elevated insulin secretion to the level of the sham-operated control rats (Tuomisto *et al.*, 1995). Our *ex vivo* experiments using the islets from TCDD-exposed mice showed that TCDD decreased the insulin level secretion significantly at 60 min after glucose stimulation, but not at 10 min [Fig. 3(A)]. This time-course pattern of insulin secretion is consistent with that of *in vivo* experiment results [Fig. 1(A)]. In summarizing the observations up to this point, TCDD exposure is thought to affect insulin secretion from the pancreatic islets mainly in the second phase.

Unlike the first phase, the second phase of insulin secretion from the islets is not regulated by a K_{ATP}-channel-dependent pathway, but possibly by a PKC pathway. The suppression of PKC was reported to cause a decrease in the glucose-stimulated insulin secretion level at 20–60 min after glucose treatment to the β cell-derived MIN6 cells (Niki *et al.*, 2003). That is, the activation of phospholipase C or inositol triphosphate induced by glucose metabolism in the mitochondria increases the level of PKC activity, and then the activated PKC will affect the K_{ATP}-channel-independent pathway. Because TCDD has been suggested to induce the translocation of PKC from the cytoplasm to the cellular membrane and to activate PKC (Kim *et al.*, 2007), it can be speculated that the TCDD-induced impairment of insulin secretion is caused by disruption of the PKC signaling pathway. The likeliness of disruption of the PKC signaling pathway by TCDD remains to be studied. On the other hand, in our *in vitro* experiment, insulin secretion was not altered despite a decrease in insulin contents in the islets by TCDD concentration as low as 0.1 nM [Fig. 4(A, B)], but the reason is not clear. We would speculate that insulin secretion could be affected by alteration of putative TCDD targets, such as glucose uptake and its metabolism, K_{ATP}-channel-regulated membrane potential and exocytosis by insulin granules rather than by insulin contents in the islets under the current experimental condition.

Most of the dioxin toxicities reported so far have been shown to be elicited in an AhR-dependent manner because these toxicities could not be observed in AhR-null mice (Gonzalez and Fernandez-Salguero, 1998; Lahvis *et al.*, 2000; Mimura *et al.*, 1997). Although the precise information on AhR target molecules is limited, it is considered that the phosphorylation of AhR is essential for the liganded AhR to bind to the xenobiotic-responsive element in the promoter region and to activate the transcription. This genomic pathway has been a dogma of AhR-mediated toxicities. On the other hand, a noncanonical theory (a 'nongenomic' pathway) has been proposed to explain the molecular mechanism of TCDD actions. In contrast to the genomic pathway, the nongenomic pathway of ligand-activated AhR does not require Arnt and activates cytosolic phospholipase A2 and Cox-2 (Dong and Matsumura, 2008), presumably by inducing a rapid increase in intracellular concentrations of Ca^{2+} within 30 min following TCDD treatment as shown in hepatic, hippocampal and epithelial cells (Hanneman *et al.*, 1996; Puga *et al.*, 1992; Tannheimer *et al.*, 1997). Thus, it is plausible to consider that the impairment of insulin secretion 60 min after TCDD exposure in our present *in vivo* and *ex vivo* experiments (Figs 1 and 3) is mainly mediated through the genomic pathway.

In the present study, we investigated the toxicity of TCDD in the pancreas using three different experimental conditions, *in vivo*, *ex vivo* and *in vitro*. Although toxicity tests using many other organs, such as liver, kidney, muscle, bone, nerve, endothelium, eye, hematopoietic cells, immune cells and macrophage have been established and utilized, no toxicity test using the pancreas has been as commonly used as these tests. A few examples using the isolated islets in toxicity studies have been documented for cadmium (Nilsson *et al.*, 1986), methylmercury (Chen *et al.*, 2006) and bisphenol (Adachi *et al.*, 2005). The apparently inconsistent observations on TCDD effects on the *in vivo*, *ex vivo* and *in vitro* experiments suggest the presence of an indirect action of TCDD to the pancreatic tissues. Thus, the utilization of combination of these three test systems is thought to be useful to study the mechanism (s) of toxicities of various chemicals in the pancreatic tissues.

In conclusion, we showed for the first time that TCDD exposure disrupts the second phase of insulin secretion from the islets and decreases the insulin contents in the islets, and that such an effect is mediated in an AhR-dependent manner. In addition, the results from the comparison among the *in vivo*, *ex vivo* and *in vitro* experiments demonstrated that TCDD affects the glucose-stimulated insulin secretion from the islets in an indirect manner, presumably via organ network.

Acknowledgments

We thank Dr Takashi Tsuboi (Department of Life Sciences, Graduate School of Arts and Sciences, The University of Tokyo) for useful advice on experiments using islets, and Drs Seiichiroh Ohsako, Masaki Kakeyama and a colleague in our laboratory for constructive comments. This work was supported in part by Global COE Program 'Medical System Innovation on Multidisciplinary Integration' from MEXT (to C.T. and H.K.), Japan.

REFERENCES

Adachi T, Yasuda K, Mori C, Yoshinaga M, Aoki N, Tsujimoto G, Tsuda K. 2005. Promoting insulin secretion in pancreatic islets by means of bisphenol A and nonylphenol via intracellular estrogen receptors. *Food Chem. Toxicol.* **43**(5): 713–719.

Aizawa T, Komatsu M. 2005. Rab27a: a new face in beta cell metabolism-secretion coupling. *J. Clin. Invest.* **115**(2): 227–230.

Bertazzi PA, Bernucci I, Brambilla G, Consonni D, Pesatori AC. 1998. The Seveso studies on early and long-term effects of dioxin exposure: a review. *Environ. Health Perspect.* **106**(suppl. 2): 625–633.

Berthoud HR, Jeanrenaud B. 1979. Acute hyperinsulinemia and its reversal by vagotomy after lesions of the ventromedial hypothalamus in anesthetized rats. *Endocrinology* **105**(1): 146–151.

Butler RA, Kelley ML, Powell WH, Hahn ME, Van Beneden RJ. 2001. An aryl hydrocarbon receptor (AHR) homologue from the soft-shell clam, *Mya arenaria*: evidence that invertebrate AHR homologues lack

2,3,7,8-tetrachlorodibenzo-*p*-dioxin and [beta]-naphthoflavone binding. *Gene* **278**(1–2): 223–234.
Chen YW, Huang CF, Tsai KS, Yang RS, Yen CC, Yang CY, Lin-Shiau SY, Liu SH. 2006. The role of phosphoinositide 3-kinase/Akt signaling in low-dose mercury-induced mouse pancreatic {beta}-cell dysfunction *in vitro* and *in vivo*. *Diabetes* **55**(6): 1614–1624.
Dong B, Matsumura F. 2008. Roles of Cytosolic Phospholipase A2 and Src kinase in the early action of 2,3,7,8-tetrachlorodibenzo-*p*-dioxin through a nongenomic pathway in MCF10A cells. *Mol. Pharmacol.* **74**(1): 255–263.
Enan E, Liu PC, Matsumura F. 1992. 2,3,7,8-Tetrachlorodibenzo-*p*-dioxin causes reduction of glucose transporting activities in the plasma membranes of adipose tissue and pancreas from the guinea pig. *J. Biol. Chem.* **267**(28): 19785–19791.
Fernandez-Salguero PM, Hilbert DM, Rudikoff S, Ward JM, Gonzalez FJ. 1996. Aryl-hydrocarbon receptor-deficient mice are resistant to 2,3,7,8-tetrachlorodibenzo-*p*-dioxin-induced toxicity. *Toxicol. Appl. Pharmacol.* **140**(1): 173–179.
Gonzalez FJ, Fernandez-Salguero P. 1998. The aryl hydrocarbon receptor. studies using the AHR-null mice. *Drug Metab. Dispos.* **26**(12): 1194–1198.
Gunton JE, Kulkarni RN, Yim S, Okada T, Hawthorne WJ, Tseng YH, Roberson RS, Ricordi C, O'Connell PJ, Gonzalez FJ, Kahn CR. 2005. Loss of ARNT/HIF1beta mediates altered gene expression and pancreatic-islet dysfunction in human type 2 diabetes. *Cell* **122**(3): 337–349.
Hahn ME, Karchner SI, Shapiro MA, Perera SA. 1997. Molecular evolution of two vertebrate aryl hydrocarbon (dioxin) receptors (AHR1 and AHR2) and the PAS family. *Proc. Natl Acad. Sci. USA* **94**(25): 13743–13748.
Hanneman WH, Legare ME, Barhoumi R, Burghardt RC, Safe S, Tiffany-castiglioni E. 1996. Stimulation of calcium uptake in cultured rat hippocampal neurons by 2,3,7,8-tetrachlorodibenzo-*p*-dioxin. *Toxicology* **112**(1): 19–28.
Henriksen GL, Ketchum NS, Michalek JE, Swaby JA. 1997. Serum dioxin and diabetes mellitus in veterans of Operation Ranch Hand. *Epidemiology* **8**(3): 252–258.
Ishida T, Kan-o S, Mutoh J, Takeda S, Ishii Y, Hashiguchi I, Akamine A, Yamada H. 2005. 2,3,7,8-Tetrachlorodibenzo-*p*-dioxin-induced change in intestinal function and pathology: evidence for the involvement of arylhydrocarbon receptor-mediated alteration of glucose transportation. *Toxicol. Appl. Pharmacol.* **205**(1): 89–97.
Ithakissios DS, Ghafghazi T, Mennear JH, Kessler WV. 1975. Effect of multiple doses of cadmium on glucose metabolism and insulin secretion in the rat. *Toxicol. Appl. Pharmacol.* **31**(1): 143–149.
Jijakli H, Malaisse WJ. 1998. Verapamil- and cadmium-resistant stimulation of calcium uptake and insulin release by -glucose in depolarised pancreatic islets exposed to diazoxide. *Cell. Signall.* **10**(9): 661–665.
Kahn SE, Hull RL, Utzschneider KM. 2006. Mechanisms linking obesity to insulin resistance and type 2 diabetes. *Nature* **444**(7121): 840–846.
Kern PA, Said S, Jackson WG, Jr., Michalek JE. 2004. Insulin sensitivity following agent orange exposure in Vietnam veterans with high blood levels of 2,3,7,8-tetrachlorodibenzo-*p*-dioxin. *J. Clin. Endocrinol. Metab.* **89**(9): 4665–4672.
Kim S-Y, Lee H-G, Choi E-J, Park K-Y, Yang J-H. 2007. TCDD alters PKC signaling pathways in developing neuronal cells in culture. *Chemosphere* **67**(9): S421–S427.
Lahvis GP, Lindell SL, Thomas RS, McCuskey RS, Murphy C, Glover E, Bentz M, Southard J, Bradfield CA. 2000. Portosystemic shunting and persistent fetal vascular structures in aryl hydrocarbon receptor-deficient mice. *Proc. Natl Acad. Sci. USA* **97**(19): 10442–10447.
Michalek JE, Pavuk M. 2008. Diabetes and cancer in veterans of Operation Ranch Hand after adjustment for calendar period, days of spraying, and time spent in Southeast Asia. *J. Occup. Environ. Med.* **50**(3): 330–340.
Michalek JE, Akhtar FZ, Kiel JL. 1999. Serum dioxin, insulin, fasting glucose, and sex hormone-binding globulin in veterans of Operation Ranch Hand. *J. Clin. Endocrinol. Metab.* **84**(5): 1540–1543.
Mimura J, Yamashita K, Nakamura K, Morita M, Takagi TN, Nakao K, Ema M, Sogawa K, Yasuda M, Katsuki M, Fujii-Kuriyama Y. 1997. Loss of teratogenic response to 2,3,7,8-tetrachlorodibenzo-*p*-dioxin (TCDD) in mice lacking the Ah (dioxin) receptor. *Genes Cells* **2**(10): 645–654.
Niki I, Niwa T, Yu W, Budzko D, Miki T, Senda T. 2003. Ca^{2+} influx does not trigger glucose-induced traffic of the insulin granules and alteration of their distribution. *Exp. Biol. Med. (Maywood)* **228**(10): 1218–1226.
Nilsson T, Rorsman F, Berggren P-O, Hellman B. 1986. Accumulation of cadmium in pancreatic [beta] cells is similar to that of calcium in being stimulated by both glucose and high potassium. *Biochim. Biophys. Acta Mol. Cell Res.* **888**(3): 270–277.
Novelli M, Piaggi S, De Tata V. 2005. 2,3,7,8-Tetrachlorodibenzo-*p*-dioxin-induced impairment of glucose-stimulated insulin secretion in isolated rat pancreatic islets. *Toxicol. Lett.* **156**(2): 307–314.
Pesatori AC, Consonni D, Bachetti S, Zocchetti C, Bonzini M, Baccarelli A, Bertazzi PA. 2003. Short- and long-term morbidity and mortality in the population exposed to dioxin after the 'Seveso accident'. *Ind. Health* **41**(3): 127–138.
Piaggi S, Novelli M, Martino L, Masini M, Raggi C, Orciuolo E, Masiello P, Casini A, De Tata V. 2007. Cell death and impairment of glucose-stimulated insulin secretion induced by 2,3,7,8-tetrachlorodibenzo-*p*-dioxin (TCDD) in the beta-cell line INS-1E. *Toxicol. Appl. Pharmacol.* **220**(3): 333–340.
Porte D, Jr. 2001. Clinical importance of insulin secretion and its interaction with insulin resistance in the treatment of type 2 diabetes mellitus and its complications. *Diabet./Metab. Res. Rev* **17**(3): 181–188.
Puga A, Nebert DW, Carrier F. 1992. Dioxin induces expression of c-fos and c-jun proto-oncogenes and a large increase in transcription factor AP-1. *DNA Cell Biol.* **11**(4): 269–281.
Schwartz GG, Il'yasova D, Ivanova A. 2003. Urinary cadmium, impaired fasting glucose, and diabetes in the NHANES III. *Diabet. Care* **26**(2): 468–470.
Tannheimer SL, Barton SL, Ethier SP, Burchiel SW. 1997. Carcinogenic polycyclic aromatic hydrocarbons increase intracellular Ca^{2+} and cell proliferation in primary human mammary epithelial cells. *Carcinogenesis* **18**(6): 1177–1182.
Thackaberry EA, Bedrick EJ, Goens MB, Danielson L, Lund AK, Gabaldon D, Smith SM, Walker MK. 2003. Insulin regulation in AhR-null mice: embryonic cardiac enlargement, neonatal macrosomia, and altered insulin regulation and response in pregnant and aging AhR-null females. *Toxicol. Sci.* **76**(2): 407–417.
Tuomisto JT, Pohjanvirta R, Unkila M, Tuomisto J. 1995. 2,3,7,8-Tetrachlorodibenzo-*p*-dioxin-induced anorexia and wasting syndrome in rats: aggravation after ventromedial hypothalamic lesion. *Eur. J. Pharmacol.* **293**(4): 309–317.
Vena J, Boffetta P, Becher H, Benn T, Bueno-de-Mesquita HB, Coggon D, Colin D, Flesch-Janys D, Green L, Kauppinen T, Littorin M, Lynge E, Mathews JD, Neuberger M, Pearce N, Pesatori AC, Saracci R, Steenland K, Kogevinas M. 1998. Exposure to dioxin and nonneoplastic mortality in the expanded IARC international cohort study of phenoxy herbicide and chlorophenol production workers and sprayers. *Environ. Health Perspect.* **106**(suppl. 2): 645–653.
Weber LWD, Stahl BU, Lebofsky M, Alper RH, Kerecsen L, Rozman K. 1991. Inhibition of phosphoenolpyruvate carboxykinase activity appears to be the key biochemical lesion in the acute toxicity of 2,3,7,8-tetrachlorodibenzo-*p*-dioxin in rats. *Chemosphere* **23**(11–12): 1957–1962.
Wild S, Roglic G, Green A, Sicree R, King H. 2004. Global Prevalence of Diabetes: Estimates for the year 2000 and projections for 2030. *Diabet. Care* **27**(5): 1047–1053.

Journal of Gastroenterology and Hepatology

JGHF

doi:10.1111/j.1440-1746.2009.06039.x

HEPATOLOGY

Adiponectin knockout mice on high fat diet develop fibrosing steatohepatitis

Takeharu Asano,* Kiyotaka Watanabe,* Naoto Kubota,† Toshiaki Gunji,* Masao Omata,* Takashi Kadowaki† and Shin Ohnishi*

*Department of Gastroenterology, †Department of Metabolic Disease, Graduate School of Medicine, University of Tokyo, Tokyo, Japan

Key words
adiponectin, animal model, high fat diet, liver fibrosis, non-alcoholic steatohepatitis.

Accepted for publication 8 February 2009.

Correspondence
Dr Shin Ohnishi, Department of Gastroenterology, Graduate School of Medicine, University of Tokyo, 7-3-1 Hongo, Bunkyo-ku, 113-8655 Tokyo, Japan. Email: sohnishi-tky@umin.ac.jp

Abstract

Background and Aim: Low levels of serum adiponectin have been reported to be associated with obesity, diabetes, and non-alcoholic steatohepatitis (NASH), as well as several malignancies. Adiponectin knockout (KO) mice have been reported to cause insulin resistance and neointimal formation of the artery. We used adiponectin KO mice fed a high fat (HF) diet, and investigated the effect of adiponectin on the progression of steatohepatitis and carcinogenesis *in vivo*.
Methods: Adiponectin KO mice and wild type (WT) mice were fed a HF diet or normal chow for the periods of 24 and 48 weeks. The HF diet contained 60% of calories from fat.
Results: The adiponectin KO mice on the HF diet showed obesity, marked elevation of serum transaminase levels, and hyperlipidemia. At 24 weeks, hepatic expression of tumor necrosis factor-α and procollagen α (I) was higher in KO mice as compared with WT mice. At 48 weeks, liver triglyceride contents in KO mice on normal chow were significantly higher than those in WT mice. Hepatocyte ballooning, spotty necrosis, and pericellular fibrosis around central veins were observed in KO mice on the HF diet. The pericellular fibrosis was more severe in KO mice on the HF diet than that in WT mice (1.62% *vs* 1.16%, $P = 0.033$). Liver adenoma and hyperplastic nodules developed in a KO mouse on the HF diet at 48 weeks (12.5%, $n = 1/8$), whereas no tumor was detected in WT mice ($n = 10$).
Conclusions: Adiponectin may play a protective role in the progression of NASH in the early stages by suppressing tumor necrosis factor-α expression and liver fibrosis.

Introduction

Non-alcoholic steatohepatitis (NASH) is thought to be a progressive disease and hepatic manifestation of the metabolic syndrome which includes insulin resistance, dyslipidemia, central obesity, and hypertension. NASH is the histological diagnosis characterized by macrovesicular steatosis, and includes inflammatory infiltration, ballooning hepatocyte, mallory's body, and varying degrees of fibrosis. A clinical study showed that about 20% of patients with NASH developed liver cirrhosis within 10 years,[1] and the cirrhotic stage of NASH appeared to be a high risk of hepatocellular carcinoma.[2,3] Moreover, steatosis accelerates the progression of fibrosis in chronic hepatitis C,[4,5] and reduces the likelihood of achieving early and sustained virologic response of interferon therapy.[6]

Adiponectin, a secreted protein derived from adipose tissue, has been reported to improve insulin resistance and hyperlipidemia,[7] and to reduce atherosclerosis.[8,9] Serum adiponectin levels are inversely correlated with body mass index of obese patients,[10] and are decreased in patients with type 2 diabetes and coronary artery disease.[11] Adiponectin increases glucose uptake and fatty acid oxidation in muscle, reduces glucose production in liver, and improves insulin sensitivity by activating adenosine 5′-monophosphate (AMP)-activated protein kinase[12] and peroxisome proliferator-activated receptor (PPAR) α.[13] Adiponectin attenuates liver fibrosis by suppressing the activity of hepatic stellate cells (HSCs) in a carbon tetrachloride-induced mouse model.[14] Tumor necrosis factor (TNF)-α is thought to be a causative factor of insulin resistance in obesity, and overexpression of TNF-α is found in the liver and in the adipose tissue of NASH patients.[15] Adiponectin inhibits TNF-α production in adipose tissue[16] as well as TNF-α-mediated activation of nuclear factor-κB signaling, and modulates the inflammatory response in vascular endothelial cells.[17]

Serum low adiponectin level has been reported to correlate with carcinogenesis of several malignancies including endometrial, breast, prostate, and colorectal cancers.[18] Regarding hepatocellular carcinoma, obesity[19] and diabetes[20] are reported to be risk factors of the cancer. High serum insulin level decreases mitochondrial β-oxidation of fatty acids, and induces inflammation and fibrosis. Adiponectin knockout (KO) mice treated with choline-deficient l-amino acid-defined diet developed liver cirrhosis and hepatic tumors.[21] Adiponectin appears to play an important role not only in the progression of NASH but also in NASH-related carcinogenesis.

There would be some differences between steatosis alone and steatohepatitis with oxidative stress and proinflammatory cytokines, and the role of adiponectin in each clinical stage has not been elucidated. To elucidate the pathophysiology of NASH, the analysis of several animal models including genetically modified models[22-26] and special diet models[27,28] has been reported. However, there is no animal model that accurately simulates the specific natural course and epidemiologic background of NASH in clinical situations.

In the present study, we used adiponectin KO mice fed a high fat (HF) diet for a long time, and investigated whether adiponectin has a physiological protective role against the progression of steatohepatitis and carcinogenesis *in vivo*.

Methods

Animals

In the present study, adiponectin KO mice have a C57Bl/6 × 129/sv genetic background. We previously reported that this animal model induced insulin resistance and glucose intolerance on normal chow, and caused neointimal formation of artery.[29] All mice used in the present study were male. Mice were provided the food and water ad libitum and were maintained on a 12 h light/dark cycle. Body weight of each mouse was measured every 2 weeks. Blood samples and liver tissues were collected from mice killed at 24 weeks (four mice per group), and 48 weeks (normal chow in WT [$n = 4$], KO [$n = 5$], and HF diet in WT [$n = 10$], KO [$n = 8$]). All animal care and experimental procedures conformed to the guidelines of the Animal Care Committee of the University of Tokyo.

High fat diet study

Mice were divided at random into two groups at 8 weeks of age. One group of mice was fed a HF diet (Nippon CLEA, Shizuoka, Japan) ad libitum, and the other was fed normal chow (Oriental Yeast, Suita, Japan). The HF diet contained 508 kcal/100 g, and 32% safflower oil, 33.1% casein, 17.6% sucrose, 5.6% cellulose. Calories from fat were 60% of total calories from the HF diet. Fatty acid of the HF diet consisted of saturated fatty acid 22% (palmitic acid 12.6%, stearic acid 8%) and unsaturated fatty acid 77% (oleic acid 64% and linoleic acid 10%). Normal chow contained 360 kcal/100 g, and 5.3% fat. Fat consisted of 13% of total calories on the HF diet. Calories per weight of HF diet were 1.4-fold those of normal chow.

Blood sample assay

Mice were fasted for > 16 h before blood sampling. Blood glucose levels were measured using an automatic blood glucose meter (Glutest Ace; Sanwa Chemical, Nagoya, Japan). Serum adiponectin levels were determined by mouse adiponectin enzyme-linked immunosorbent assay (ELISA) kit (Otsuka Pharmaceutical, Tokyo, Japan). Serum aspartate aminotransferase (AST), alanine aminotransferase (ALT), total cholesterol (TC), non-esterified fatty acid (NEFA), and triglyceride (TG) levels were determined by a transaminase CII-test, TC *E*-test, NEFA *C*-test, TG *E*-test (Wako Pure Chemical Industries, Osaka, Japan), respectively.

Liver TG content

Liver homogenates were extracted, and tissue triglyceride content was determined as described previously with an extract solution (chloroform : methanol = 2:1).[30]

Reverse transcription-polymerase chain reaction

Total RNA was prepared from liver tissue with TRIzol Reagent (Invitrogen, Carlsbad, CA, USA) according to the manufacturer's instructions. The RNA levels corresponding to various target genes were quantified using a polymerase chain reaction (PCR)-based technique. The extracted RNA was converted into cDNA by reverse transcription (TaqMan reverse transcription reagents, Applied Biosystems, Foster City, CA, USA). The cDNA solutions were analyzed by TaqMan technology, a real-time PCR assay (TaqMan PCR reagent kit, Applied Biosystems). Specific gene expression was quantified by real time PCR carried out on an ABI Prism 7900HT (Applied Biosystems). RNA expression of β-actin was measured as an internal control. Relative expression levels of target genes were compared after normalization to β-actin.

Histological analysis

Liver tissues were fixed with 10% formalin and embedded in paraffin. Cross-sections (5 μm thick) were cut and stained with hematoxylin and eosin (H&E). The extent of liver fibrosis was evaluated with Masson trichrome stain by the reported technique.[31,32] Areas around the central veins were chosen and quantitatively evaluated on sections stained with Masson trichrome for collagen. Thirty areas from a cross-section of each animal were digitized with a global magnification of ×200. Area calculations were based on measurements made with image editing (Photoshop, San Jose, CA, USA) and image analysis (Scion Image, Frederick, MD, USA) programs.

Statistical analysis

Results were expressed as mean ± standard deviation (SD). Differences of continuous data between groups were examined for statistical significance using Student's *t*-test (Stat View, Cary, NC, USA). Data were considered statistically significant at a $P < 0.05$.

Results

Mice on HF diet gradually gained weight

The appearance and body weight was similar between the wild type (WT) mice and the KO mice on the HF diet (Fig. 1a). On the HF diet, body weights in both mice groups were significantly heavier than those on normal chow, and increased from 24 to 48 weeks (Fig. 1b).

Effect of HF diet on serum adiponectin levels

The serum adiponectin levels in WT mice on the HF diet tended to decrease (65%) from 24 to 48 weeks ($P = 0.097$), whereas mice on normal chow showed very small interval change (Fig. 2a). The serum adiponectin levels of KO mice were below detection limits.

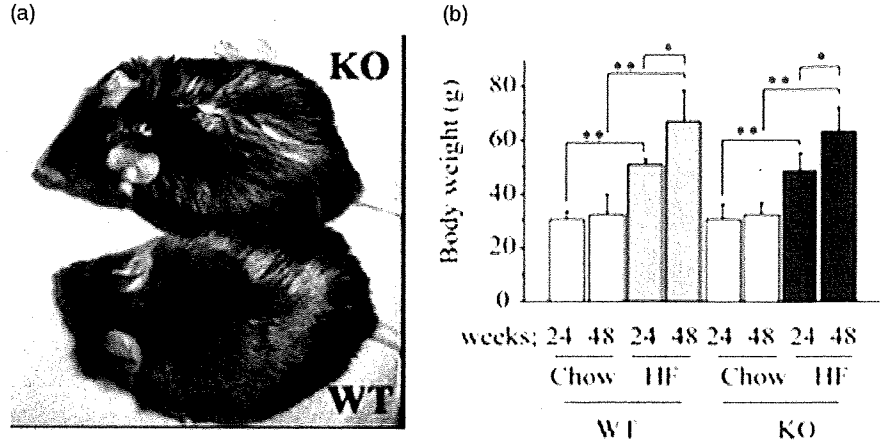

Figure 1 Mice on the high fat (HF) diet showed obesity. (a) The photograph shows wild type (WT) mice and knockout (KO) mice on the HF diet at 48 weeks. The appearances were similar between WT and adiponectin KO mice. (b) Body weights are shown at 24 and 48 weeks in WT and adiponectin KO mice. Each value is mean ± standard deviation (SD), significance at $*P < 0.05$, $**P < 0.01$.

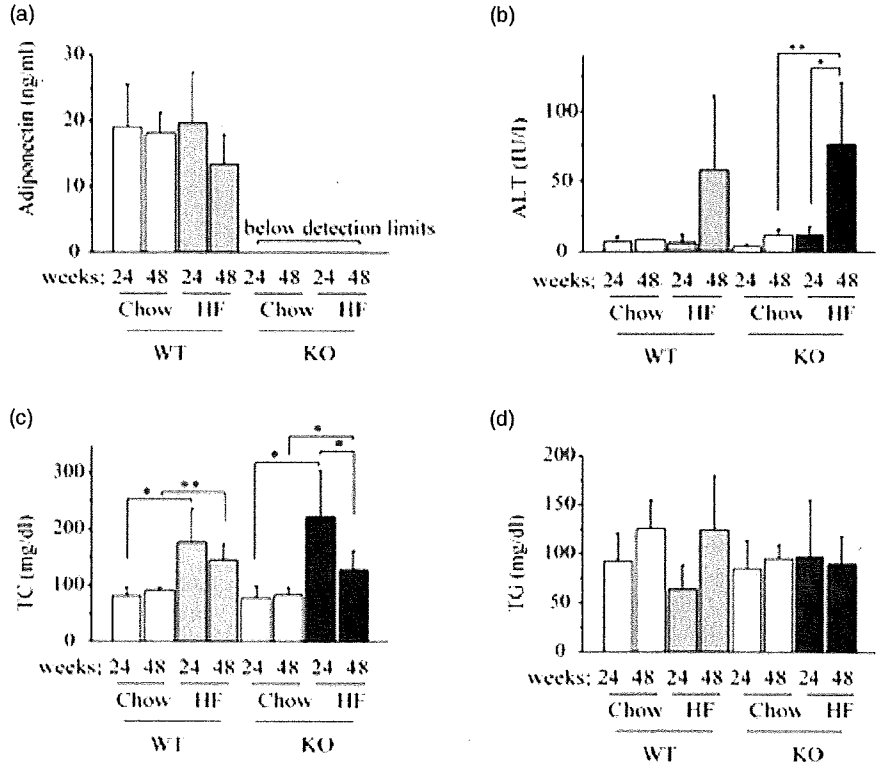

Figure 2 Mice on the high fat (HF) diet showed hyperglycemia, hyperlipidemia, and transaminase elevation. Serum levels of (a) adiponectin, (b) alanine aminotransferase (ALT), (c) total cholesterol (TC), and (d) triglyceride (TG) were measured in wild type (WT) and adiponectin knockout (KO) mice at 24 and 48 weeks. Each value is mean ± standard deviation (SD), significance at $*P < 0.05$, $**P < 0.01$.

Serum transaminase and lipid levels in adiponectin KO mice

The blood glucose levels in both WT and KO mice on the HF diet were significantly higher than that of mice on normal chow (data not shown). Serum ALT levels in KO mice on the HF diet were significantly higher than that of mice on normal chow at 48 weeks (Fig. 2b), and AST levels were similar. Serum TC levels were significantly higher in both WT and KO mice on the HF diet than that of mice on normal chow at 24 weeks (Fig. 2c). Serum TG levels in WT mice tended to increase from 24 to 48 weeks (Fig. 2d). Serum NEFA (data not shown), TC, TG levels were similar between WT and KO mice.

Liver TG contents in adiponectin KO mice

The liver of mice on the HF diet was enlarged and homogeneously white in color (Fig. 3a). The liver TG contents in KO mice on normal chow were significantly higher than that of WT mice at 48 weeks, although there was no significant difference between WT and KO mice on the HF diet (Fig. 3b).

Hepatic RNA expression of TNF-α was significantly higher in adiponectin KO mice

At 24 weeks, hepatic RNA expression of TNF-α in KO mice on the HF diet was significantly higher by threefold than that in WT mice

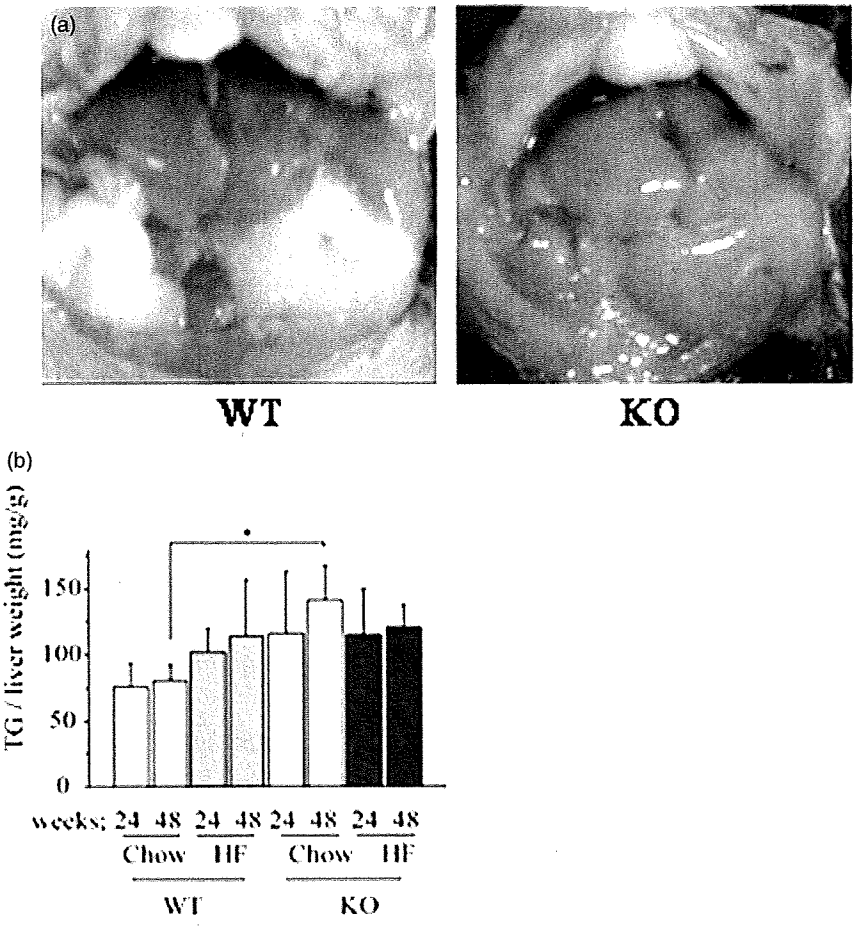

Figure 3 Liver triglyceride (TG) contents in Adiponectin knockout (KO) mice on normal chow were significantly higher as compared with wild type (WT) mice. (a) The photograph shows livers of WT mice and adiponectin KO mice on the high fat (HF) diet at 48 weeks. The appearances of liver were similar between WT and KO mice. (b) The liver TG contents were measured in WT and adiponectin KO mice at 24 and 48 weeks. Each value is the mean ± standard deviation (SD), significance at $*P < 0.05$, $**P < 0.01$.

($P = 0.03$) (Fig. 4a). The expression of procollagen α (I) in KO mice on the HF diet was higher by fourfold than that in WT mice at 24 weeks (Fig. 4b). The expression of lipogenic genes such as Sterol Regulatory Element-binding Protein (SREBP)-1c, stearoyl Co-A desaturase-1 (SCD1) was significantly higher on the HF diet in both WT and KO mice than that in mice on normal chow (data not shown). The expression of cyclin D1 in KO mice on the HF diet was significantly higher than that in mice on normal chow, and it tended to be higher by 1.5-fold that in WT mice at 48 weeks (Fig. 4c).

Adiponectin KO mice showed steatohepatitis with pericellular fibrosis

In histopathological analysis of mice on normal chow, hepatic tissue appeared almost normal at 24 weeks and 48 weeks in WT mice, and at 24 weeks in KO mice. Some KO mice on normal chow at 48 weeks showed mild lipid accumulation around central veins. The liver of WT and KO mice on HF diet showed massive hepatocyte ballooning around central veins, but almost no fibrosis was detected by Masson trichrome staining (Fig. 5a). At 48 weeks, KO mice showed lobular lipid accumulation, prominent hepatocyte ballooning, spotty necrosis, Mallory body, eosinophilic focus, and notable pericellular fibrosis (Fig. 5b). According to human NASH criteria reported by Brunt *et al.* these features were matched to Grade 3, Stage 1. Hepatic fibrosis areas around central veins were quantitatively evaluated, and the fibrosis in KO mice was more severe than that in WT mice at 48 weeks (1.16 ± 0.4% *vs* 1.62 ± 0.43%, respectively, $P = 0.033$) (Fig. 5c).

Adenoma developed in the liver of an adiponectin KO mouse at 48 weeks

A liver tumor of 10 mm in diameter was detected in one of the KO mice (12.5%, $n = 1/8$) at 48 weeks (Fig. 6a). The tumor contained a large fat deposit with mild atypia, and was diagnosed as liver adenoma (Fig. 6b,c). Histology of other small nodular lesions that were detected in the same mouse was regenerative hyperplastic alteration. In contrast, no tumor was detected in the livers of WT mice ($n = 10$).

Discussion

In the present study, adiponectin KO mice on the HF diet showed steatosis, inflammation, fibrosis, and tumor formation, which are well recognized as pathological features specific for NASH. The mice had taken the HF diet that did not contain chemicals promoting liver fibrosis such as endotoxin or carbon tetrachloride, and thus are considered to be an animal model of NASH.

Several animal models of NASH have been advocated to date. Methionine-choline deficient diet and the choline-deficient L-amino acid-defined diet model showed steatosis, liver fibrosis, and liver tumors, without obesity.[28] Mice fed the HF liquid diet by

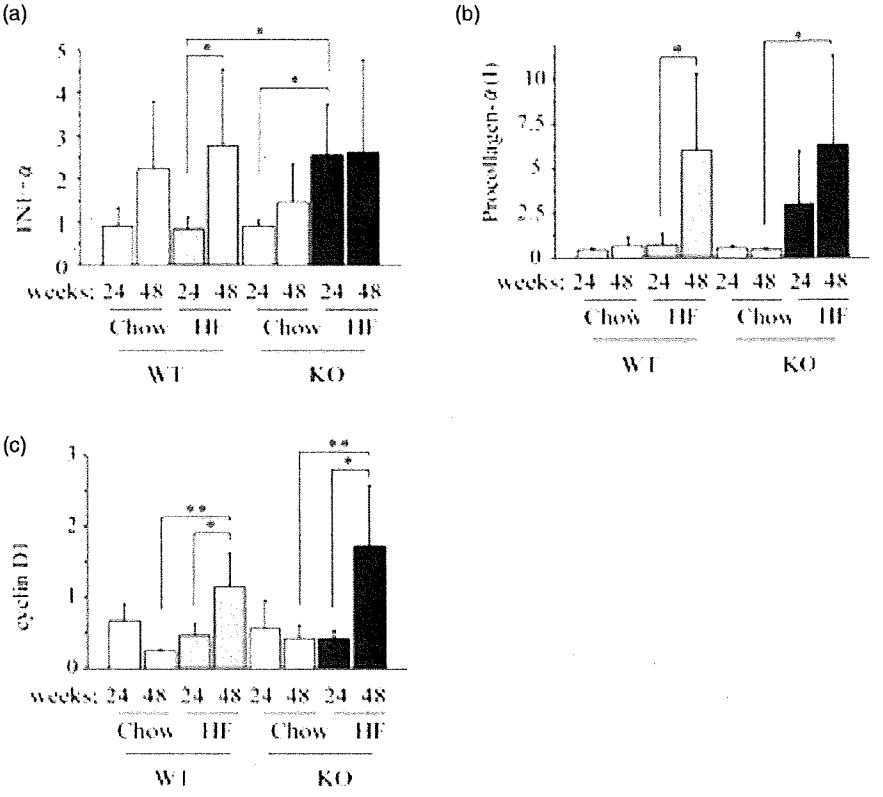

Figure 4 Hepatic expression of tumor necrosis factor-α (TNF-α) was significantly higher in adiponectin knockout (KO) mice. Hepatic RNA expression levels of (a) TNF-α, (b) procollagen α (I), and (c) cyclin D1 were measured in wild type (WT) and adiponectin KO mice at 24 and 48 weeks. Each value is mean ± standard deviation (SD), significance at $*P < 0.05$, $**P < 0.01$.

implanted gastrostomy tube induced NASH without liver tumor.[27] Liver-specific PTEN KO mice showed macrovesicular steatosis, liver fibrosis, and tumors.[26] However, there has been no report of mouse model developing NASH on a HF diet alone. HF composition is epidemiologically considered one of the main causes of obesity and NASH. Clinical study in humans requires a lengthy amount of time to estimate fibrosis or progression in the natural course of NASH. Therefore, we used the animal model and estimated outcomes during the limited period. We chose adiponectin KO mice because NASH is commonly associated with hypoadiponectinemia in humans.[33] We hope this model will provide beneficial clues to clinical studies of diet therapy or drug development for obesity and steatohepatitis.

Some of the KO mice on normal chow at 48 weeks showed mild lipid accumulation around the central veins, and the liver TG contents were significantly higher than that of WT mice. KO mice were susceptible to liver TG accumulation on normal chow. However, there was no significant difference of liver TG contents between KO mice and WT mice on the HF diet. There might be a limit of liver TG accumulation volume for a certain period. These features might resemble the state of 'burned-out' NASH in which the lipid accumulation and inflammation become unremarkable in the progressed NASH patient.[34]

Hepatic expression of TNF-α was significantly higher in adiponectin KO mice on the HF diet at 24 weeks (early stage), and maintained a high level until 48 weeks (late fibrotic stage). TNF-α induces insulin resistance by inhibiting the tyrosine phosphorylation of insulin receptor substance-1,[35] and would lead to a vicious circle of escalating steatosis. On the other hand, TNF-α has functions of inducing apoptosis, and attenuating the resistance against necrosis. Adiponectin KO mice on a HF diet at 48 weeks showed hepatic spotty necrosis and Mallory body, which indicated liver injury. Adiponectin inhibits TNF-α production in adipose tissue[16] and TNF-α-mediated activation of nuclear factor-κB signaling through a cAMP-dependent pathway.[17] In the liver, the majority of TNF-α is produced by Kupffer cells. Alcoholic steatohepatitis has been reported to enhance Kupffer cells sensitization to endotoxin (lipopolysaccharide), and increase TNF-α production.[36] Also in NASH patients, it is hypothesized that the liver might be highly susceptible to adipocytokines from intraperitoneal massive adipose tissue and endotoxine from the intestinal tract.

The expression of procollagen α (I) as well as TNF-α was higher at 24 weeks, and subsequent hepatic fibrosis was significantly promoted at 48 weeks in adiponectin KO mice on the HF diet as compared with the WT mice. TNF-α induces activation of HSC directly and stimulates production of transforming growth factor (TGF)-β. HSC plays central roles in liver fibrosis with TGF-β and collagens.[37] TGF-β is a main mediator of proliferation and migration for HSC, and activated HSC enhances the expression of procollagen α, which is the target gene of TGF-β. Thus, adiponectin might suppress not only TNF-α mediated inflammation, but also TNF-α-induced liver fibrosis. Elevation of TNF-α in the early stage may indicate HSC activation and fibrosis at a late stage. At 48 weeks, serum adiponectin in WT mice tended to be decreased, so the difference in TNF-α and procollagen might be little between WT and KO mice. Kamada *et al.* reported that the carbon tetrachloride administered adiponectin KO mice showed extensive liver fibrosis with activation of HSC and overexpression of TGF-β1. Notably, the fibrosis was improved by supplementation of

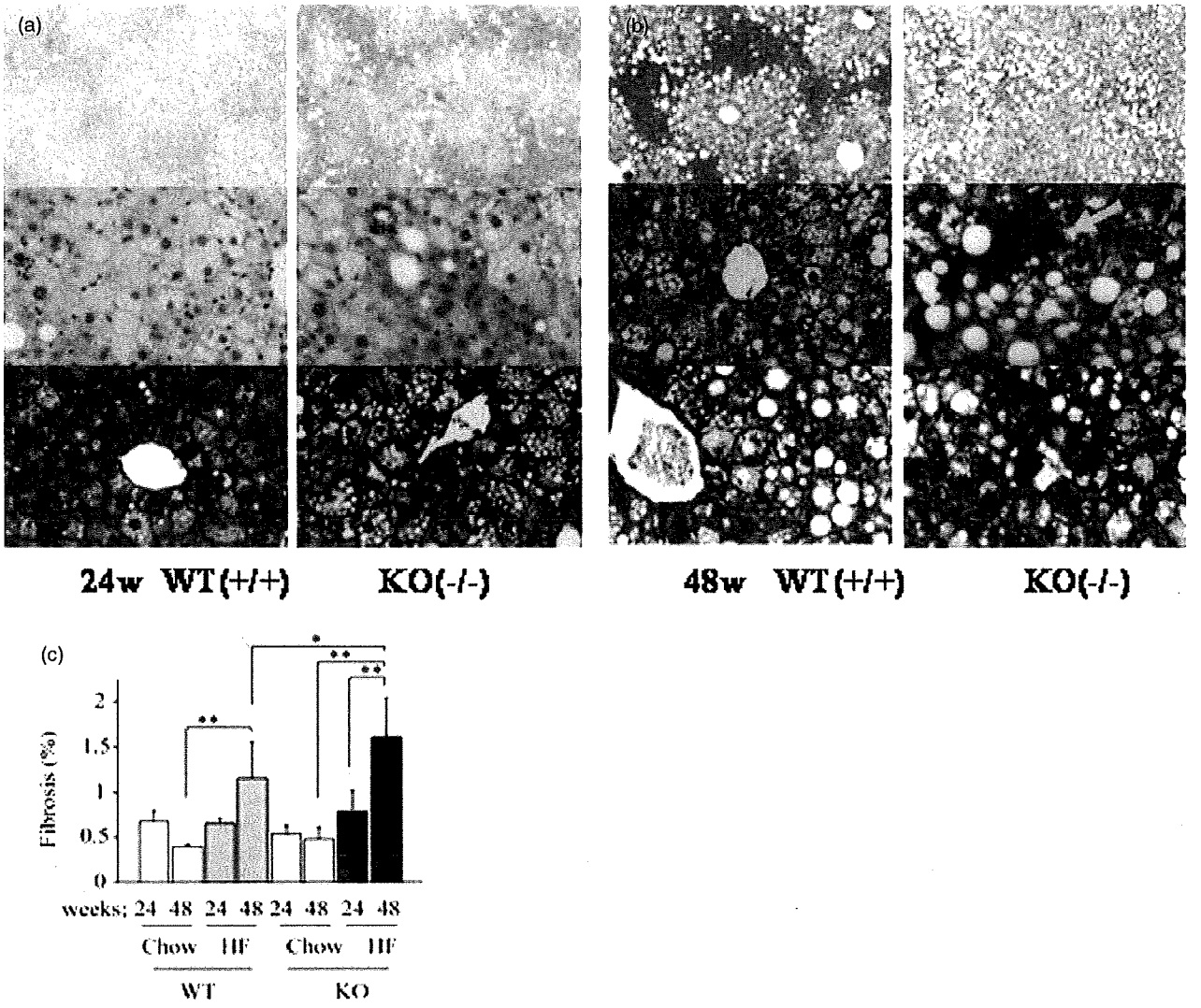

Figure 5 Adiponectin knockout (KO) mice showed steatohepatitis. (a) The liver sections of wild type (WT) and adiponectin KO mice on the high fat (HF) diet at 24 weeks. The first and second rows show a lower (×40) and higher (×200) magnification of hematoxylin and eosin (H&E)-stained livers, respectively. Hepatocyte ballooning was observed around central veins. Liver fibrosis was not detected by Masson trichrome staining in either model (third row, magnifications ×200). (b) The liver sections of WT and adiponectin KO mice on the HF diet at 48 weeks. The first and second rows show a lower (×40) and higher (×200) magnification of H&E-stained livers, respectively. Adiponectin KO mice showed lobular lipid accumulation, hepatocyte ballooning, spotty necrosis (arrow) and especially pericellular fibrosis around the central veins as determined by Masson trichrome staining (third row, magnifications ×200). (c) Hepatic fibrosis areas around the central veins were measured in WT and adiponectin KO mice at 24 and 48 weeks. Each value is mean ± standard deviation (SD), significance at $*P < 0.05$, $**P < 0.01$.

adiponectin.[14] Thus, adiponectin is considered to play a protective role against liver fibrosis by suppressing TNF-α expression.

Peroxisome proliferator-activated receptor γ is primarily localized to HSC, and PPARγ agonist inhibits proliferation and activation of human HSC.[38] Evidence of improvement to NASH was demonstrated by use of PPARγ agonist. PPARγ agonist improved insulin resistance and histological features including fibrosis.[39] The action of PPARγ agonist has been reported to occur with adiponectin dependently in the liver and adiponectin independently in skeletal muscle.[40]

A liver adenoma was detected in one of the adiponectin KO mice on the HF diet at 48 weeks, though any tumor was not detected in WT mice. In the present study, KO mice have a C57Bl/6 × 129/sv genetic background that rarely develops into liver tumor.[41] CDAA diet in adiponectin KO mice was reported to accelerate liver tumor formation.[21] Recently, it has been more frequently reported that hepatocellular carcinoma in patients with cryptogenic cirrhosis might be associated with NASH.[2,42] Larger prospective clinical studies of patients with NASH are needed to establish the risk of carcinogenesis.

Hepatic expression of cyclin D1 was higher in adiponectin KO mice on the HF diet at 48 weeks. Cyclin D1 is thought to play a critical role in transition from the G1 to S Phase of the cell cycle. The overexpression of cyclin D1 can provoke a perturbed

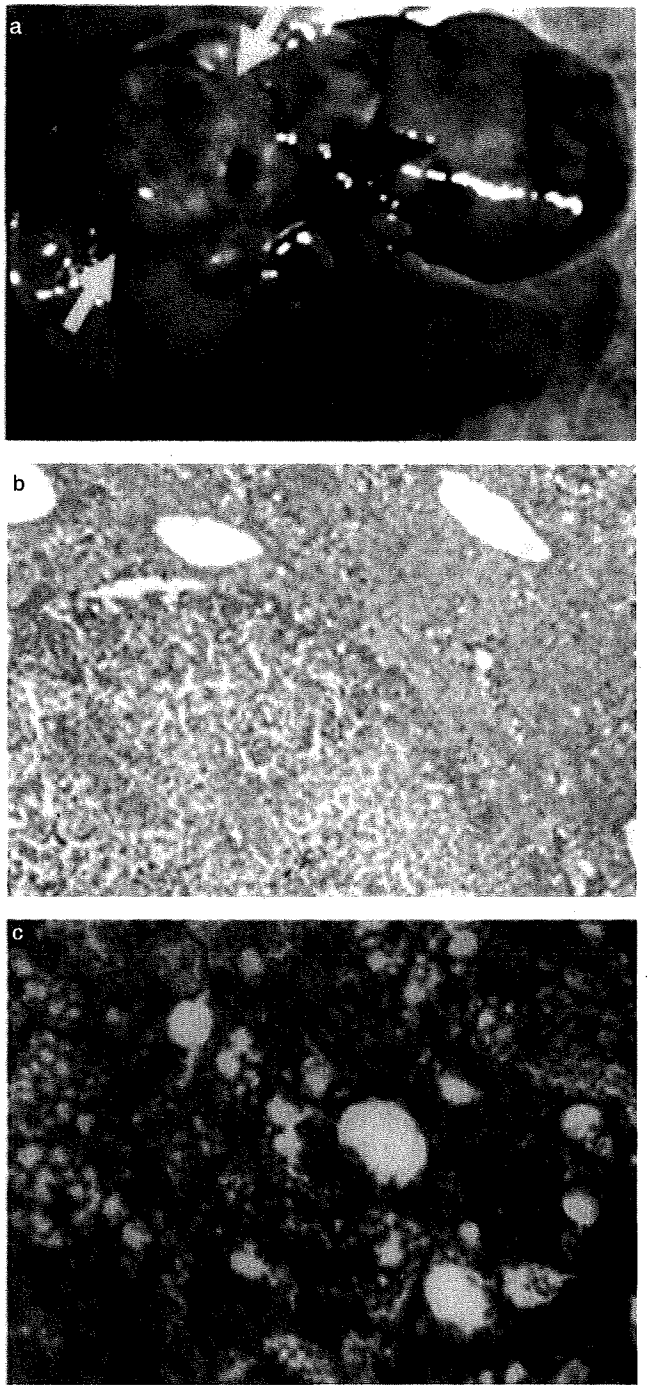

Figure 6 Liver adenoma was observed in an adiponectin knockout (KO) mouse. (a) A liver tumor of 10 mm in diameter was observed (arrow) in one of the adiponectin KO mice (12.5%, $n = 1/8$) at 48 weeks. The tumor had grown pressing surrounded normal liver architecture and partially protruding from the liver. (b) Hematoxylin and eosin (H&E)-stained section of the liver tumor in (a). The tumor hepatocytes contained large amounts of fat deposits. The border between the tumor and surrounding normal liver parenchyma is clear. (c) H&E-stained section of the liver tumor with mild atypia, diagnosed as adenoma. Magnifications are ×40 (b), ×200 (c).

progression of the G1 phase of the cell cycle. Rearrangement, amplification, and overexpression of the cyclin D1 gene have been detected in several types of cancers, including esophageal, breast, and liver cancers.[43,44] Microvesicular steatosis and hepatocellular carcinoma with overexpression of cyclin D1 was observed in retinoic acid receptor-α dominant negative form transgenic mouse, and the carcinogenesis was considered to be caused by Wnt signal activation with loss of retinoic acid signal.[25] Hepatic steatosis is frequently observed in hepatitis C virus (HCV)-infected patients. Analysis of HCV core gene transgenic mice suggested that hepatocarcinogenesis in HCV infection may be associated with mitochondrial dysfunction, reactive oxygen species overproduction,[45] enhanced expression of TNF-α, activation of activator protein-1,[46] and activation of retinoic acid receptor-α.[47] The mechanism of carcinogenesis in NASH still remains uncertain. Therefore, experimental study in the NASH model would require a further examination including genetic analysis.

In conclusion, adiponectin KO mice on a HF diet for a prolonged period induced obesity, hyperlipidemia, steatohepatitis, pericellular fibrosis, and adenoma formation. These mice showed natural history and features very similar to the pathogenesis of NASH in human. Adiponectin may play a protective role against the progression of NASH in the early stage by suppression of TNF-α expression and liver fibrosis. Deficiency of adiponectin may participate in liver carcinogenesis related to steatohepatitis.

Acknowledgments

The present study was supported by the Program of Fundamental Studies in Health Sciences of the National Institute of Biomedical Innovation (NIBIO), by the NFAT project of New Energy and Industrial Technology Development Organization (NEDO) and by the Special Coordination Fund for Science and Technology from the Ministry of Education, Culture, Sports, Science and Technology, Japan.

References

1 Matteoni CA, Younossi ZM, Gramlich T, Boparai N, Liu YC, McCullough AJ. Nonalcoholic fatty liver disease: a spectrum of clinical and pathological severity. *Gastroenterology* 1999; **116**: 1413–9.
2 Bugianesi E, Leone N, Vanni E *et al.* Expanding the natural history of nonalcoholic steatohepatitis: from cryptogenic cirrhosis to hepatocellular carcinoma. *Gastroenterology* 2002; **123**: 134–40.
3 Marrero JA, Fontana RJ, Su GL, Conjeevaram HS, Emick DM, Lok AS. NAFLD may be a common underlying liver disease in patients with hepatocellular carcinoma in the United States. *Hepatology* 2002; **36**: 1349–54.
4 Hourigan LF, Macdonald GA, Purdie D *et al.* Fibrosis in chronic hepatitis C correlates significantly with body mass index and steatosis. *Hepatology* 1999; **29**: 1215–19.
5 Adinolfi LE, Gambardella M, Andreana A, Tripodi MF, Utili R, Ruggiero G. Steatosis accelerates the progression of liver damage of chronic hepatitis C patients and correlates with specific HCV genotype and visceral obesity. *Hepatology* 2001; **33**: 1358–64.
6 Patton HM, Patel K, Behling C *et al.* The impact of steatosis on disease progression and early and sustained treatment response in chronic hepatitis C patients. *J. Hepatol.* 2004; **40**: 484–90.

7 Yamauchi T, Kamon J, Minokoshi Y *et al.* Adiponectin stimulates glucose utilization and fatty-acid oxidation by activating AMP-activated protein kinase. *Nat. Med.* 2002; **8**: 1288–95.
8 Matsuda M, Shimomura I, Sata M *et al.* Role of adiponectin in preventing vascular stenosis. The missing link of adipo-vascular axis. *J. Biol. Chem.* 2002; **277**: 37 487–91.
9 Okamoto Y, Kihara S, Ouchi N *et al.* Adiponectin reduces atherosclerosis in apolipoprotein E-deficient mice. *Circulation* 2002; **106**: 2767–70.
10 Arita Y, Kihara S, Ouchi N *et al.* Paradoxical decrease of an adipose-specific protein, adiponectin, in obesity. *Biochem. Biophys. Res. Commun.* 1999; **257**: 79–83.
11 Hotta K, Funahashi T, Arita Y *et al.* Plasma concentrations of a novel, adipose-specific protein, adiponectin, in type 2 diabetic patients. *Arterioscler. Thromb. Vasc. Biol.* 2000; **20**: 1595–9.
12 Yamauchi T, Kamon J, Waki H *et al.* The fat-derived hormone adiponectin reverses insulin resistance associated with both lipoatrophy and obesity. *Nat. Med.* 2001; **7**: 941–6.
13 Yamauchi T, Kamon J, Waki H *et al.* Globular adiponectin protected ob/ob mice from diabetes and ApoE-deficient mice from atherosclerosis. *J. Biol. Chem.* 2003; **278**: 2461–8.
14 Kamada Y, Tamura S, Kiso S *et al.* Enhanced carbon tetrachloride-induced liver fibrosis in mice lacking adiponectin. *Gastroenterology* 2003; **125**: 1796–807.
15 Crespo J, Cayon A, Fernandez Gil P *et al.* Gene expression of tumor necrosis factor alpha and TNF-receptors, p55 and p75, in nonalcoholic steatohepatitis patients. *Hepatology* 2001; **34**: 1158–63.
16 Maeda N, Shimomura I, Kishida K *et al.* Diet-induced insulin resistance in mice lacking adiponectin/ACRP30. *Nat. Med.* 2002; **8**: 731–7.
17 Ouchi N, Kihara S, Arita Y *et al.* Adiponectin, an adipocyte-derived plasma protein, inhibits endothelial NF-kappaB signaling through a cAMP-dependent pathway. *Circulation* 2000; **102**: 1296–301.
18 Kelesidis I, Kelesidis T, Mantzoros CS. Adiponectin and cancer: a systematic review. *Br. J. Cancer* 2006; **94**: 1221–5.
19 Calle EE, Rodriguez C, Walker Thurmond K, Thun MJ. Overweight, obesity, and mortality from cancer in a prospectively studied cohort of U.S. adults. *N. Engl. J. Med.* 2003; **348**: 1625–38.
20 El Serag HB, Tran T, Everhart JE. Diabetes increases the risk of chronic liver disease and hepatocellular carcinoma. *Gastroenterology* 2004; **126**: 460–8.
21 Kamada Y, Matsumoto H, Tamura S *et al.* Hypoadiponectinemia accelerates hepatic tumor formation in a nonalcoholic steatohepatitis mouse model. *J. Hepatol.* 2007; **47**: 556–64.
22 Fan CY, Pan J, Usuda N, Yeldandi AV, Rao MS, Reddy JK. Steatohepatitis, spontaneous peroxisome proliferation and liver tumors in mice lacking peroxisomal fatty acyl-CoA oxidase. Implications for peroxisome proliferator-activated receptor alpha natural ligand metabolism. *J. Biol. Chem.* 1998; **273**: 15639–45.
23 Lu SC, Alvarez L, Huang ZZ *et al.* Methionine adenosyltransferase 1A knockout mice are predisposed to liver injury and exhibit increased expression of genes involved in proliferation. *Proc. Natl Acad. Sci. USA* 2001; **98**: 5560–5.
24 Martinez Chantar ML, Corrales FJ, Martinez Cruz LA *et al.* Spontaneous oxidative stress and liver tumors in mice lacking methionine adenosyltransferase 1A. *FASEB J.* 2002; **16**: 1292–4.
25 Yanagitani A, Yamada S, Yasui S *et al.* Retinoic acid receptor alpha dominant negative form causes steatohepatitis and liver tumors in transgenic mice. *Hepatology* 2004; **40**: 366–75.
26 Horie Y, Suzuki A, Kataoka E *et al.* Hepatocyte-specific Pten deficiency results in steatohepatitis and hepatocellular carcinomas. *J. Clin. Invest.* 2004; **113**: 1774–83.
27 Deng QG, She H, Cheng JH *et al.* Steatohepatitis induced by intragastric overfeeding in mice. *Hepatology* 2005; **42**: 905–14.
28 Koteish A, Diehl AM. Animal models of steatosis. *Semin. Liver Dis.* 2001; **21**: 89–104.
29 Kubota N, Terauchi Y, Yamauchi T *et al.* Disruption of adiponectin causes insulin resistance and neointimal formation. *J. Biol. Chem.* 2002; **277**: 25863–6.
30 Murakami K, Tobe K, Ide T *et al.* A novel insulin sensitizer acts as a coligand for peroxisome proliferator-activated receptor-alpha (PPAR-alpha) and PPAR-gamma: effect of PPAR-alpha activation on abnormal lipid metabolism in liver of Zucker fatty rats. *Diabetes* 1998; **47**: 1841–7.
31 Caballero T, Perez Milena A, Masseroli M *et al.* Liver fibrosis assessment with semiquantitative indexes and image analysis quantification in sustained-responder and non-responder interferon-treated patients with chronic hepatitis C. *J. Hepatol.* 2001; **34**: 740–7.
32 Ikura Y, Ohsawa M, Shirai N *et al.* Expression of angiotensin II type 1 receptor in human cirrhotic livers: Its relation to fibrosis and portal hypertension. *Hepatol. Res.* 2005; **32**: 107–16.
33 Hui JM, Hodge A, Farrell GC, Kench JG, Kriketos A, George J. Beyond insulin resistance in NASH: TNF-alpha or adiponectin? *Hepatology* 2004; **40**: 46–54.
34 Caldwell SH, Oelsner DH, Iezzoni JC, Hespenheide EE, Battle EH, Driscoll CJ. Cryptogenic cirrhosis: clinical characterization and risk factors for underlying disease. *Hepatology* 1999; **29**: 664–9.
35 Hotamisligil GS, Spiegelman BM. Tumor necrosis factor alpha: a key component of the obesity-diabetes link. *Diabetes* 1994; **43**: 1271–8.
36 Enomoto N, Takei Y, Hirose M *et al.* Thalidomide prevents alcoholic liver injury in rats through suppression of Kupffer cell sensitization and TNF-alpha production. *Gastroenterology* 2002; **123**: 291–300.
37 Friedman SL. Seminars in medicine of the Beth Israel Hospital, Boston. The cellular basis of hepatic fibrosis. Mechanisms and treatment strategies. *N. Engl. J. Med.* 1993; **328**: 1828–35.
38 Galli A, Crabb D, Price D *et al.* Peroxisome proliferator-activated receptor gamma transcriptional regulation is involved in platelet-derived growth factor-induced proliferation of human hepatic stellate cells. *Hepatology* 2000; **31**: 101–8.
39 Promrat K, Lutchman G, Uwaifo GI *et al.* A pilot study of pioglitazone treatment for nonalcoholic steatohepatitis. *Hepatology* 2004; **39**: 188–96.
40 Kubota N, Terauchi Y, Kubota T *et al.* Pioglitazone ameliorates insulin resistance and diabetes by both adiponectin-dependent and -independent pathways. *J. Biol. Chem.* 2006; **281**: 8748–55.
41 Stevens LC, Little CC. Spontaneous testicular teratomas in an inbred strain of Mice. *Proc. Natl Acad. Sci. USA* 1954; **40**: 1080–7.
42 Ratziu V, Bonyhay L, Di Martino V *et al.* Survival, liver failure, and hepatocellular carcinoma in obesity-related cryptogenic cirrhosis. *Hepatology* 2002; **35**: 1485–93.
43 Hunter T, Pines J. Cyclins and cancer. II: Cyclin D and CDK inhibitors come of age. *Cell* 1994; **79**: 573–82.
44 Zhang YJ, Jiang W, Chen CJ *et al.* Amplification and overexpression of cyclin D1 in human hepatocellular carcinoma. *Biochem. Biophys. Res. Commun.* 1993; **196**: 1010–16.
45 Moriya K, Nakagawa K, Santa T *et al.* Oxidative stress in the absence of inflammation in a mouse model for hepatitis C virus-associated hepatocarcinogenesis. *Cancer Res.* 2001; **61**: 4365–70.
46 Tsutsumi T, Suzuki T, Moriya K *et al.* Alteration of intrahepatic cytokine expression and AP-1 activation in transgenic mice expressing hepatitis C virus core protein. *Virology* 2002; **304**: 415–24.
47 Tsutsumi T, Suzuki T, Shimoike T *et al.* Interaction of hepatitis C virus core protein with retinoid X receptor alpha modulates its transcriptional activity. *Hepatology* 2002; **35**: 937–46.

The Prostate 69:644 – 651 (2009)

Suppression of Prostate Cancer in a Transgenic Rat Model Via γ-Tocopherol Activation of Caspase Signaling

Satoru Takahashi,[1]* Kentaro Takeshita,[1] Azman Seeni,[1] Satoshi Sugiura,[1] Mingxi Tang,[1] Shin-ya Sato,[1] Hiroki Kuriyama,[2] Masao Nakadate,[2] Koichi Abe,[3] Yoshitaka Maeno,[4] Masataka Nagao,[4] and Tomoyuki Shirai[1]

[1]*Department of Experimental Pathology and Tumor Biology, Mizuho-ku, Nagoya, Japan*
[2]*Tama Biochemical Co. Ltd, Isehara, Kanagawa, Japan*
[3]*Eisai Co. Ltd., Bunkyo-ku, Tokyo, Japan*
[4]*Forensic Medical Science, Nagoya City University Graduate School of Medical Sciences, Nagoya, Japan*

BACKGROUND. Epidemiological data indicate that intake of one form of vitamin E, γ-tocopherol, may reduce prostate cancer risk, and several in vitro studies have demonstrated that γ-tocopherol can inhibit prostate cancer cell growth. The purpose of the present study was to confirm effects of γ-tocopherol on prostate cancer in the transgenic rat for adenocarcinoma of prostate (TRAP) model established in our laboratory.

METHODS. In Experiment 1, heterozygous male TRAP rats 5 weeks of age received α-tocopherol at the concentration of 50 mg/kg in the diet, or γ-tocopherol at 50 or 100 mg/kg for 10 weeks. In Experiment 2, TRAP rats of 3 weeks of age were given γ-tocopherol at 50, 100, or 200 mg/kg diet for 7 weeks.

RESULTS. γ-Tocopherol did not affect body weight gain, organ weights or serum levels of either testosterone or estradiol. However, quantitative evaluation of prostatic lesions demonstrated significantly suppression of sequential progression from PIN to adenocarcinoma in a dose-dependent manner, along with clear activation of caspases 3 and 7 in the ventral lobe in both experiments.

CONCLUSIONS. The present study clearly demonstrated that γ-tocopherol suppresses prostate tumor progression in an in vivo TRAP model, and could be a candidate chemopreventive agent for human prostate cancer. *Prostate 69: 644–651, 2009.* © 2009 Wiley-Liss, Inc.

KEY WORDS: **γ-tocopherol; prostate cancer; transgenic rat model, chemoprevention**

INTRODUCTION

Prostate cancer has become the most common malignancy in men in Europe and the United States while its incidence remains relatively low in Asian countries [1]. It has been estimated there were approximately 232,090 new cases of prostate cancer and 30,350 deaths from prostate cancer in the United States in 2005 [2]. Prevalence of prostate cancer has also been increasing in Japan [3], concomitantly with change in life style. Androgen ablation therapy is widely accepted and carried out for prostate cancers because androgens are essential for the development and growth of normal prostate and prostate cancer cells

Azman Seeni's present address is School of Dental Sciences, Universiti Sains Malaysia, 16150 Kubang Kerian, Kelantan, Malaysia.

Masataka Nagao's present address is Department of Legal Medicine, Graduate School of Biomedical Sciences, Hiroshima University, Hiroshima, Japan.

*Correspondence to: Satoru Takahashi, 1 Kawasumi, Mizuho-cho, Mizuho-ku, Nagoya 467-8601, Japan.
E-mail: sattak@med.nagoya-cu.ac.jp
Received 25 September 2008; Accepted 5 December 2008
DOI 10.1002/pros.20915
Published online 13 January 2009 in Wiley InterScience (www.interscience.wiley.com).

[4]. However, outgrowth of hormone-independent cancer cells occurs within 1–2 years and eventually leads to a fatal outcome in many cases [5].

Chemoprevention is one attractive approach for prostate cancer because of the high population incidence and long latent period, and several dietary factors as well as genetic background have been linked to risk and progression of prostate cancer [6–8]. Prostate cancer is known to be strongly associated with aging, that is, about three-quarters of cases worldwide occur in men aged 65 years or more [1]. Therefore, the main strategy with chemoprevention for prostate cancer is to delay the development of clinically evident disease due to suppression of progression from precancerous lesions to invasive cancer. Many observational or intervention studies have been conducted using vitamins, phytochemicals and minerals [5]. α- and γ-Tocopherols, forms of vitamin E, are nutritional elements that may reduce risk of prostate cancer [9–13]. To confirm effects of γ-tocopherol in vivo, we here performed animal experiments using the transgenic rat for adenocarcinoma of prostate (TRAP) model that features development of high-grade prostatic intraepithelial neoplasia (PIN) from 4 weeks of age and well—moderately differentiated adenocarcinomas with high incidences by 15 weeks of age [14,15]. These characteristics of TRAP have been shown to be very suitable for evaluation of strategies for chemoprevention and treatment [16–19].

MATERIALS AND METHODS

Chemicals and Animals

Vitamin E-free, α- or γ-tocopherol-contained diets were donated by Tama Biochemical Co. Ltd. (Japan). Antibodies for caspases 3, 6, 7, 9, cleaved caspases 3, 7, Erk1/2, phospho-Erk1/2, p38 MAPK, phospho-p38 MAPK, SAPK/JNK, and phospho-SAPK/JNK were purchased from Cell Signaling Technology (Beverly, MA). Anti-AR (PG-21) was from Upstate Technology (Lake Placid, NY, CA), anti-cyclin D1 was from Oncogene Research Product, anti-Bcl-xL was from Pharmingen, anti-SV40T Ag was from Santa Cruz Biotechnology, Inc. and anti-β-actin was from Sigma–Aldrich, Inc. Male heterozygous TRAP rats with a Sprague–Dawley genetic background were bred in our animal facility for use in the present study. They were housed 2–3/cage on wood-chip bedding in an air-conditioned animal room at 23 ± 2°C and 50 ± 10% humidity. Food and tap water were available ad libitum.

Experimental Protocol

Experiment 1. A total of 40 male TRAP rats aged 5 weeks were randomly divided into four groups. Rats of group 1 as a control received vitamin E-free AIN73 basal diet. The rats of groups 2–4 continuously received α-tocopherol at the concentration of 50 mg/kg diet, or γ-tocopherol at the concentrations of 50 or 100 mg/kg diet for 10 weeks, respectively. The experiment was terminated at week 10.

Experiment 2. A total of 56 heterozygous male TRAP rats aged 3 weeks were randomly divided into four groups. Rats of group 1 served as a control receiving vitamin E-free AIN73 basal diet. The rats of groups 2, 3, and 4 continuously received γ-tocopherol-containing AIN73 at the concentrations of 50, 100, or 200 mg/kg diet for 7 weeks, respectively. The experiment was terminated at week 7.

In both experiments, prostates were removed and fixed in formalin. Portions were immediately frozen in liquid nitrogen and stored at −80°C until processed. Testosterone and estrogen levels in serum were analyzed using radioimmunoassays by a commercial laboratory (SRL, Inc., Tokyo, Japan). The present experiments were performed under protocols approved by the Institutional Animal Care and Use Committee of Nagoya City University Graduate School of Medical Sciences.

Assessment of Prostate Neoplastic Lesion Development

Neoplastic lesions in prostate glands of TRAP rats were evaluated as previously described [18]. Briefly, neoplastic lesions were classified into three types; low-grade PIN (LG-PIN), high-grade PIN (HG-PIN) and adenocarcinoma. The relative numbers of acini with the relevant histological characteristics were quantified by counting, the results being expressed relative to the total acini in each prostatic lobe.

Immunoblot Analysis

Frozen ventral prostate tissues were homogenized in RIPA buffer (150 mM NaCl, 50 mM Tris–HCl (pH 8.0), 1% NP-40, 0.5% sodium deoxycholate, 0.1% SDS, 1 mM phenylmethylsulphonyl fluoride, 1 mM sodium orthovanadate, and protease inhibitor cocktail (Complete, Roche)). Twenty microgram aliquots of protein were resolved on SDS–PAGE and separated proteins were transferred to nitrocellulose membranes for detection with horseradish peroxidase conjugated secondary antibodies and the ECL Plus system (Amersham Pharmacia Biotech).

Determination of Total Ceramide Content

The frozen tissues of ventral prostates were homogenized in twenty parts of chloroform/methanol (2:1) containing 250 ng of C_2-ceramide as an internal

standard and extracted for 30 min on ice. After centrifugation, the chloroform phase was dried under a nitrogen stream. The amount of C_{16}-ceramide in tissue was quantified by high-performance liquid chromatography/electro-spray ionization mass spectrometry (LC/MS) as described by Soeda et al. [20].

HPLC Method for the Determination of Tocopherols in Rat Plasma

Tocopherols are extracted from 0.5 ml of plasma with 5.0 ml of n-hexane after addition of 0.7 ml of water and 1.0 ml of ethanol containing dl-Tocol (3.92 μg/ml) as an internal standard. Hexane extracts (4 ml) are evaporated under a nitrogen stream at 40°C and residues were dissolved in 100 μl aliquots of n-Hexane. The resultant solutions were applied to a high-performance liquid chromatography column (Nucleosil-100 Å 5 μm NH2, 4.6 mm × 250 mm; elution, n-Hexane/isopropyl alcohol = 98:2).

Immunohistochemistry

For Ki-67 immunostaining, deparaffinized sections were incubated with diluted rabbit polyclonal Ki-67 antibodies (Novocastra, New Castle, UK). Apoptotic cells were detected using an In situ Apoptosis Detection Kit (TUNEL method) according to the manufacturer's instructions (Takara Bio Co. Ltd, Japan). Labeling indices were counted separately in the ventral, dorsal and lateral prostate and expressed as numbers of Ki-67-positive or TUNEL-positive cells per 100 cells.

Statistical Analysis

Differences in means between groups were determined by analysis of variance (ANOVA), followed by the Scheffe's post-hoc test with StatView (version 5.0) software (SAS Institute, Inc., Cary, NC). The Spearman's rank correlation coefficient test was used for analysis of dependent data.

RESULTS

Experiment I

α- and γ-Tocopherol did not influence the mean body weights and relative liver and ventral prostate weights (Table I). Serum levels of testosterone and estradiol were also not affected (Fig. 1A). There were partial pathological responses to γ-tocopherol as demonstrated by reduction in the prostatic neoplastic lesions in TRAP rats (Fig. 1B). However, small foci of adenocarcinoma still remained, so that there were no significant differences in the incidences of PIN or adenocarcinomas in the prostates of TRAP rats. Quantitative evaluation of the proportion of preneoplastic and neoplastic lesions in prostate glands showed γ-tocopherol to significantly suppress progression from PIN to adenocarcinoma in a dose-dependent manner in the ventral lobe while α-tocopherol was without apparent influence (Table II). In the lateral lobe, γ-tocopherol treatment also tended to suppress progression but this was not significant. Immunoblot analyses showed activation of caspases 3 and 7, inactivation of Erk1/2 and decreased expression of bcl-2 in the ventral prostate of rats treated with γ-tocopherol while expression of cyclin D1 and SV40 T antigen did not differ among the groups (Fig. 2). There was no variation in ceramide content in the ventral prostate among the groups (Fig. 1C).

Experiment 2

To confirm the reproducibility of the suppressive effects of γ-tocopherol on prostate carcinogenesis, we performed a similar experiment as in Experiment 1. γ-Tocopherol did not affect either body weight gain or organ weights (Table III). Serum levels of testosterone and estradiol again did not differ among the groups (Fig. 3A). Serum concentrations of γ-tocopherol were increased in a dose-dependent manner while the α-tocopherol level was not affected (Fig. 3B). Prostate adenocarcinomas were found only in ventral and lateral lobes and no intergroup differences in incidences were observed. However, progressive

TABLE I. Final Body and Relative Organ Weights (Experiment I)

Treatment	No. of rats	Body weight (g)	Relative organ weight (%)	
			Liver	Ventral prostate
Control	10	463.7 ± 34.7	3.27 ± 0.24	0.056 ± 0.014
α-Tocopherol 50 mg/kg	10	448.6 ± 40.1	3.22 ± 0.15	0.064 ± 0.007
γ-Tocopherol 50 mg/kg	10	455.0 ± 28.9	3.39 ± 0.21	0.060 ± 0.009
γ-Tocopherol 100 mg/kg	10	445.7 ± 39.0	3.47 ± 0.28	0.060 ± 0.008

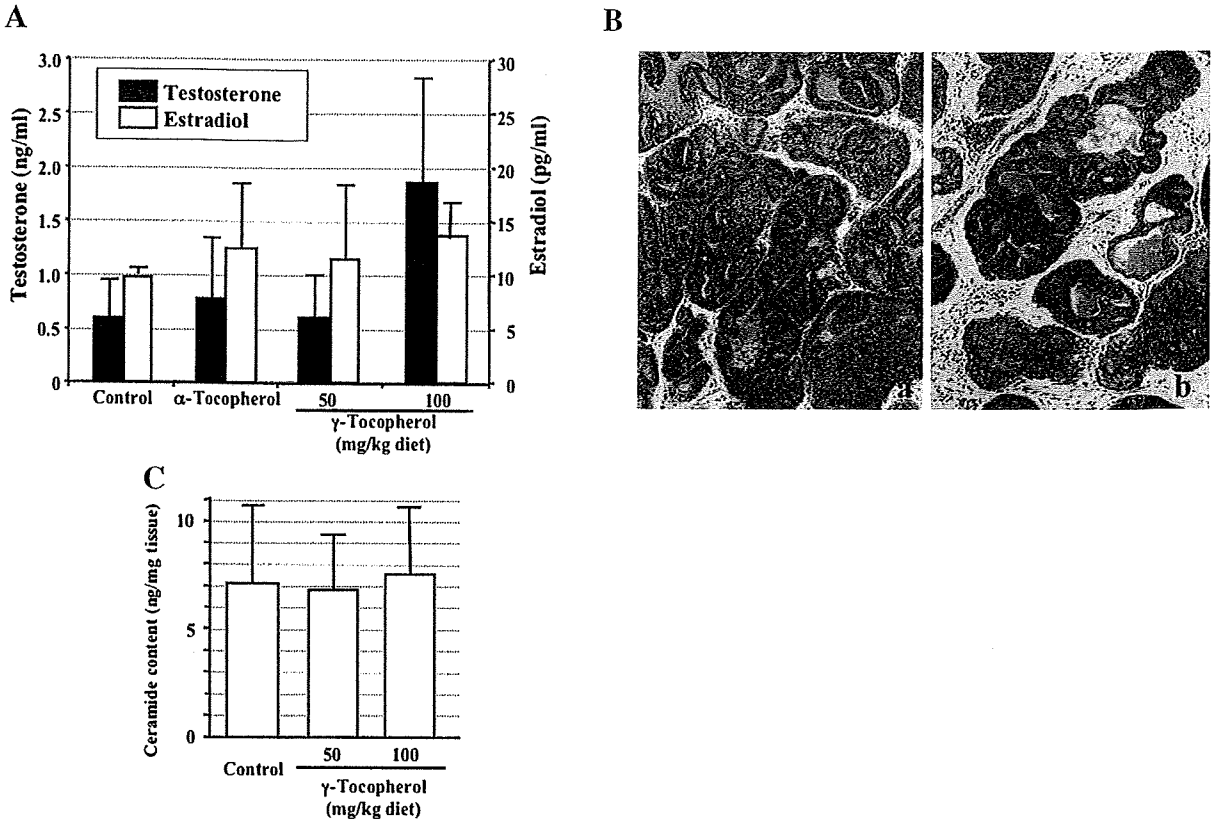

Fig. 1. Effects of γ-tocopherol on serum steroid hormones, prostatic lesions and ceramide content in prostate glands in Experiment I. **A**: Serum levels of testosterone and estradiol. **B**: Representative histopathological findings for lesions in the ventral prostates of the controls (a) and the 100 mg/kg γ-tocopherol group (b). **C**: Ceramide contents in ventral prostates.

changes of prostatic lesions showed a significant suppression by γ-tocopherol in a dose-dependent manner in the ventral but not the lateral lobe (Table IV). The numbers of apoptotic cells in the ventral prostate of rats treated with γ-tocopherol were significantly increased in a dose-dependent manner as compared with the controls whereas there were no obvious differences in Ki-67 labeling indices (Fig. 3C,D). Immunoblot analyses clearly demonstrated activation of caspases 3 and 7 and a tendency for inactivation of Erk1/2 in the ventral prostate of rats treated with γ-tocopherol (Fig. 4).

TABLE II. Quantitative Evaluation of Neoplastic Lesions in Prostates of TRAP RatsTreated With α- and γ-Tocopherol (Experiment I)

		Relative number of acini with histological characteristics (%)					
		Ventral lobe			Lateral lobe		
Treatment	No. of rats	LG-PIN	HG-PIN	ADC	LG-PIN	HG-PIN	ADC
Control	10	5.4 ± 2.5	87.5 ± 2.4	7.2 ± 2.3	14.2 ± 3.9	84.4 ± 3.6	1.4 ± 1.3
α-Tocopherol 50 mg/kg	10	8.6 ± 2.9	85.4 ± 1.8	6.0 ± 1.9	16.5 ± 8.7	82.3 ± 8.3	1.2 ± 0.9
γ-Tocopherol 50 mg/kg	10	8.1 ± 3.1	86.9 ± 3.5	5.0 ± 1.8[b]	19.4 ± 6.5	79.9 ± 6.7	0.7 ± 0.8
γ-Tocopherol 100 mg/kg	10	9.8 ± 4.9	85.4 ± 4.4	4.7 ± 1.0[a,b]	15.9 ± 5.8	83.5 ± 5.8	0.6 ± 0.7

LG-PIN, low grade prostatic intraepithelial neoplasia; HG, high grade; ADC, adenocarcinoma.
[a] $P < 0.05$ versus control.
[b] $P < 0.01$ versus control (Spearman's rank correlation coefficient test).

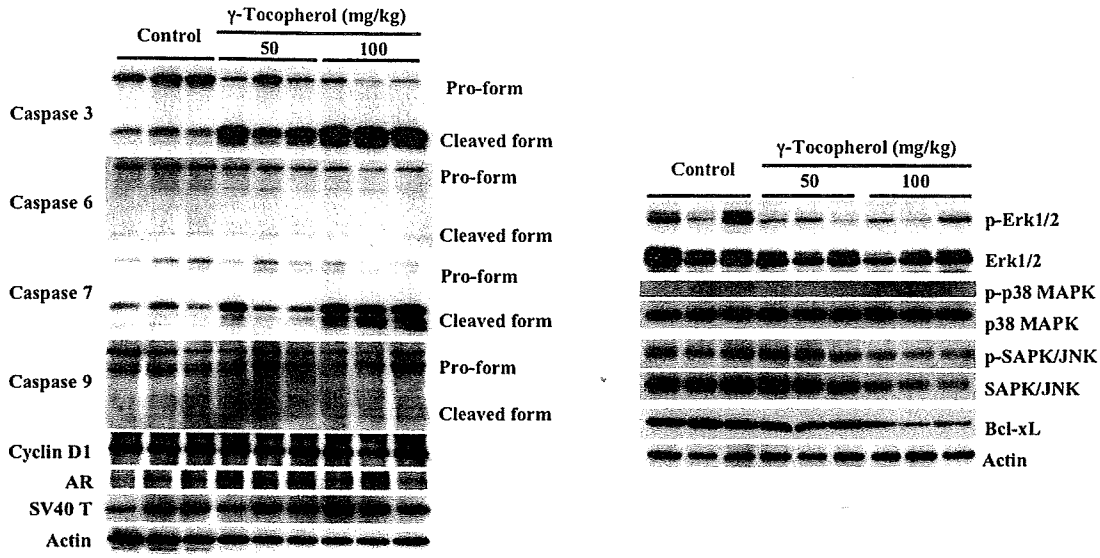

Fig. 2. Results of immunoblot analysis of caspases, MAPKs and other apoptosis-related proteins in ventral prostates of TRAP rats treated with γ-tocopherol in Experiment I.

DISCUSSION

To our knowledge, this is the first study to demonstrate suppression effects of γ-tocopherol on prostate tumor progression in an in vivo animal model. Various mechanisms whereby the compound could inhibit prostate cancer cell growth have been indicated in in vitro studies, including downregulation of cyclins D1 and E [21,22] or induction of apoptosis by interrupting sphingolipid synthesis [23]. The data from our TRAP model also point to induction of apoptosis via activation of caspases 3 and 7 by γ-tocopherol although downregulation of cyclin D1 and significant accumulation of ceramide were not found.

It has been reported that Japanese men intake an average of 12.2 ± 2.1 mg γ-tocopherol per day in daily life [24]. The amount of γ-tocopherol used in the highest-dose group (200 mg/kg diet) of present study was 50–60 times higher than this human exposure level and was equivalent to an intake of 950 mg/day by a 70 kg-sized human. However, it is possible to consume this amount of γ-tocopherol in nutritional supplements.

Vitamin E is composed of eight structurally related forms, four tocopherols and four tocotrienols. α-Tocopherol is found as the highest concentration in serum and dietary supplements among all isoforms but the primary form in the typical American diet is γ-tocopherol, which is present at 2–4 times higher concentrations than α-tocopherol [25]. Although both α- and γ-tocopherol are potent antioxidants, γ-tocopherol has a unique function due to its different chemical structure that scavenges reactive nitrogen species that damage proteins, lipids, and DNA. Therefore, γ-tocopherol possesses electrophile-trapping and nitrogen dioxide-radical-trapping properties that are different from those of α-tocopherol [26,27]. Consequently, γ-tocopherol appears to have greater efficacy than α-tocopherol at inhibiting lipid peroxidation under nitration system conditions [28]. Furthermore, γ-tocopherol but not α-tocopherol exhibits anti-inflammatory activities by inhibiting cyclooxygenase-catalyzed prostaglandin E_2 formation in cell culture and in animals in vivo [29,30]. Recent clinical trials revealed no significant reduction of overall cardiovascular events or cancer by α-tocopherol

TABLE III. Final Body and Relative Organ Weights (Experiment 2)

			Relative organ weights (%)			
Treatment	No. of rats	Body weights (g)	Liver	Kidneys	Heart	Ventral prostate
Control	14	347.5 ± 42.4	4.06 ± 0.29	0.68 ± 0.03	0.32 ± 0.01	0.065 ± 0.009
γ-Tocopherol 50 mg/kg	14	353.3 ± 35.9	4.18 ± 0.30	0.70 ± 0.04	0.33 ± 0.02	0.066 ± 0.010
γ-Tocopherol 100 mg/kg	14	343.5 ± 41.1	3.97 ± 0.24	0.69 ± 0.03	0.33 ± 0.01	0.063 ± 0.007
γ-Tocopherol 200 mg/kg	14	340.5 ± 27.0	3.86 ± 0.31	0.69 ± 0.04	0.33 ± 0.02	0.060 ± 0.009